



NIH Public Access

Author Manuscript

Q Rev Biophys. Author manuscript; available in PMC 2013 September 03.

Published in final edited form as:

Q Rev Biophys. 2012 August ; 45(3): 345–381. doi:10.1017/S0033583512000078.

Structure and mechanism of purine binding riboswitches

Robert T. Batey

Department of Chemistry and Biochemistry, University of Colorado at Boulder, Campus Box 215, Boulder, Colorado 80309-0215, USA

Abstract

A riboswitch is a non-protein coding sequence capable of directly binding a small molecule effector without the assistance of accessory proteins to regulate expression of the mRNA in which it is embedded. Currently, over 20 different classes of riboswitches have been validated in bacteria with the promise of many more to come, making them an important means of regulation of the genome in the bacterial kingdom. Strikingly, half of the known riboswitches recognize effector compounds that contain a purine or related moiety. In the last decade significant progress has been made to determine how riboswitches specifically recognize these compounds against the background of many other similar cellular metabolites and transduce this signal into a regulatory response. Of the known riboswitches, the purine family containing guanine, adenine, and 2'-deoxyguanosine binding classes are the most extensively studied, serving as a simple and useful paradigm for understanding how these regulatory RNAs function. This review provides a comprehensive summary of the current state of knowledge regarding the structure and mechanism of these riboswitches, as well as insights into how they might be exploited as therapeutic targets and novel biosensors.

1. Introduction

One of the most significant discoveries of the post-genomic era is the extent to which RNA plays a role in regulating normal cellular homeostasis and guiding physiological responses to changes in environment or extracellular cues such as hormones (Couzin, 2002). While significant attention has been given to the numerous RNAs involved in eukaryotic interference mechanisms (Ghildiyal & Zamore, 2009), new classes of RNAs continue to be discovered, such as long noncoding RNAs (lncRNAs) that further expand our knowledge of RNA-mediated control of cellular programs (Wang & Chang, 2011). In bacteria, an extensive set of non-coding RNAs and regulatory elements have also been characterized (Gripenland et al., 2010; Storz et al., 2011). These RNAs include protein-binding elements, transcriptional and translational attenuators, temperature and pH sensors, metabolite sensors, and cis- and trans-acting antisense RNAs. Even a form of RNA interference is present in bacteria that is mediated by small CRISPR-derived RNAs and used as an antiviral defense mechanism (Barrangou et al., 2007; Deveau et al., 2010). A major challenge in biology remains the discovery and characterization of the complete set of these RNAs, somewhat accurately called the “dark matter of biology” (Blaxter, 2010). Towards this goal, substantial progress has been made in the last decade on understanding the structure and mechanisms of *riboswitches*, an RNA-based regulatory element broadly distributed throughout the bacterial kingdom, and more sparsely in archaea, plants, and fungi (Barrick & Breaker, 2007).

Riboswitches are defined as cis-acting elements found within an mRNA non-protein coding region that regulates expression through its ability to specifically and directly bind a small

molecule (Breaker, 2011). A typical riboswitch consists of two functional domains: a small molecule receptor (called the *aptamer domain*) and a regulatory domain (called the *expression platform*) (Garst & Batey, 2009; Winkler & Breaker, 2003). The receptor is a highly folded structure that specifically binds an effector molecule, typically a metabolite directly related to the genes encoded by the mRNA containing that riboswitch. For example, purine family riboswitches mostly, but not exclusively, regulate genes involved in purine biosynthesis or transport (Mandal et al., 2003; Mandal & Breaker, 2004a). Currently over 20 classes of riboswitches have been validated that contain receptors that respond to nucleobases and nucleosides, amino acids, cofactors, aminosugars, and metal ions (Breaker, 2011). In addition, there are at least that many “orphan” motifs that are suspected to be riboswitches, but have no known effector (Barrick et al., 2004; Weinberg et al., 2007; Weinberg et al., 2010). Half of the known riboswitch receptors interact with effector molecules that contain a purine moiety. These include members of a group that bind nucleotide derivatives (guanine, adenine, 2'-deoxyguanosine, cyclic-di-GMP, and preQ₁) and members of another group that bind coenzymes (*S*-adenosylmethionine, *S*-adenosylhomocysteine, and adenosylcobalamin). This review will focus on members of the first group.

It is perhaps not surprising that many of these effector molecules contain a purine nucleobase as a component for several reasons. Yarus has proposed that AMP-bearing cofactors such as nicotinamide adenine dinucleotide (NAD⁺) and flavin adenine dinucleotide (FAD) are the descendants of the initial Darwinian ancestors (IDA) that gave rise to the subsequent RNA world (Yarus, 2011). Other ancient cofactors such as *S*-adenosylmethionine (SAM), coenzyme A, and ATP that are clearly traceable to the last universal common ancestor (LUCA) and likely to have been present in the hypothesized RNA world all bear an adenosyl moiety (Benner et al., 1989). If riboswitches are ancient holdovers from this world (Blouin et al., 2009; Vitreschak et al., 2004), then recognition of these purine-bearing compounds is certain to have been important for ancient RNAs. From a modern perspective, on the other hand, specific recognition of purine nucleobases and nucleotides through a diverse set of base-base interactions observed in biological RNAs (Leontis & Westhof, 1998; Leontis & Westhof, 2001) can be achieved by informationally simple motifs (Carothers et al., 2004). For example, the “classic” ATP aptamer (Sassanfar & Szostak, 1993) has emerged multiple times across independent experiments (Saran et al., 2003). Currently, there are a number of structurally distinct ATP and GTP aptamers that exhibit a diverse range of both affinity and specificity, indicating many solutions exist to the problem of recognizing purines and their derivatives (Huang & Szostak, 2003; Sazani et al., 2004; Weill et al., 2004).

The regulatory domain of riboswitches are always found downstream of the receptor and most often contain a switch consisting of two overlapping and mutually exclusive secondary structures that direct the expression machinery (Garst & Batey, 2009). For example, an archetypal riboswitch that regulates at the transcriptional level contains two hairpin structures in this domain (Fig. 1). One is an intrinsic (rho-independent) terminator--a stem-loop followed by a uridine tract (Fig. 1, top)--that directs RNA polymerase (RNAP) to disengage from the nascent transcript using a well-established mechanism (Peters et al., 2011). Conversely, this domain can form an “anti-terminator” (Fig. 1, bottom) that disrupts terminator formation, thereby allowing the polymerase to pass through the leader and into the coding sequence and allowing for expression of the encoded protein. At the heart of this mechanism is a *switching sequence* (Fig. 1, red), typically found at the boundary of the two domains, which partitions to either the aptamer (generally the first or “P1” helix) or the expression platform, dictating the fate of the mRNA. Riboswitches can employ a number of regulatory mechanisms, including translational attenuation, antisense, and alternative splicing (Breaker, 2010). The secondary structural switch is not exclusive to riboswitches,

but is a broadly utilized mechanism in RNA. It was first appreciated in the regulation of tryptophan biosynthesis in *Bacillus subtilis* by the *trp* RNA-binding attenuation protein (TRAP) (Kuroda et al., 1988; Shimotsu et al., 1986), and more recently was identified in a regulatory element of the human VEGFA mRNA (Ray et al., 2009). Thus, riboswitches tap into a broad form of RNA-mediated regulation in which signal input is achieved through a variety of mechanisms that direct a secondary structural switch.

Following the validation of the first riboswitches (McDaniel et al., 2003; Mironov et al., 2002; Nahvi et al., 2002), their structural and biophysical characterization has provided the bulk of our current understanding of their function. These studies have focused upon several major questions. First, how are riboswitch receptors structured to create a specific and high affinity binding site for a small molecule? Currently, every family of purine-binding riboswitch, with the notable exception of the adenosylcobalamin family, has some high resolution structural information associated with it. Secondly, ligand-directed formation of alternative secondary structures in the regulatory domain suggests that RNA folding is a critical component of riboswitch function. How do riboswitches efficiently acquire both secondary and tertiary architecture necessary to carry out their regulatory function? Third, how does binding of ligand to the receptor get communicated to the downstream regulatory domain to elicit the appropriate expression response? Finally, how can we translate our structural and biophysical understanding of riboswitches to real world applications? In this review, each of these questions will be specifically addressed using the purine binding riboswitches to illustrate, as these, and in particular, the guanine/adenine binding classes, are the dominant model systems.

2. Structural basis for recognition of purines by riboswitches

2.1 The purine riboswitch family: guanine/adenine classes

The guanine/adenine classes of the purine riboswitch family were identified as a conserved sequence in the leaders of the *ydhL* and *xpt-pbuX* operons of *B. subtilis* that terminate transcription in the presence of hypoxanthine or guanine (Christiansen et al., 1997; Johansen et al., 2003). This level of regulation is in addition to control at the DNA level by a classic repressor mechanism involving the PurR protein that when bound by hypoxanthine or guanine, binds DNA and blocks transcription (Saxild et al., 2001). Biochemical analysis of the *xpt-pbuX* leader sequence demonstrated that this RNA operates by directly binding guanine, hypoxanthine, or xanthine to direct the downstream secondary structural switch (Mandal et al., 2003). Association of guanine with the mRNA without the assistance of a protein was demonstrated using a combination of equilibrium dialysis, “in-line” chemical probing of the RNA structure (Regulski & Breaker, 2008), and analysis of compensatory base pairing mutations. This set of experimental approaches has now been applied by the Breaker group to many distinct riboswitches, and currently represents an accepted and robust path to the validation of newly discovered riboswitches. Subsequent to validation of the guanine riboswitch, an adenine-binding class of riboswitches was discovered (Mandal & Breaker, 2004b).

The guanine and adenine classes share a common secondary structure centered upon a three-way junction (Mandal et al., 2003; Mandal & Breaker, 2004a). Three helices (P1, P2, and P3) form the Watson-Crick base paired regions of the RNA, and contain very little sequence conservation beyond the need to base pair (Fig. 2a). Conserved nucleotides are instead clustered in the two terminal hairpin loops (L2 and L3) and the joining regions between the three helices (J1/2, J2/3, and J3/1). The pattern of conserved nucleotides in the loops suggested a possible pseudoknot interaction in which base pairs would be formed between the two loops (Mandal et al., 2003; Mandal & Breaker, 2004a). While conservation patterns within both loops indicate that these nucleotides are functionally important, it is the three-

way junction that was directly implicated in ligand recognition. First, in-line chemical probing showed the greatest differences in RNA structure between the bound and unbound forms in the three-way junction (Mandal et al., 2003). Guanine, hypoxanthine, and xanthine induce protection of these regions of the RNA from self-cleavage in the presence of magnesium, indicating that the junction becomes more structured upon ligand binding. Conversely, the loops displayed no ligand-dependent behavior. Second, it was noted that nucleotide 74 in J3/1 (Fig. 2a) is always a cytosine in the guanine class and always a uridine in the adenine class, suggesting that a Watson-Crick pair is formed between the nucleobase ligand and the RNA (Mandal et al., 2003; Mandal & Breaker, 2004a).

Crystal structures of the *B. subtilis* *xpt-pbuX* guanine riboswitch (Batey et al., 2004; Serganov et al., 2004) and the *Vibrio vulnificus* *add* adenine riboswitch (Serganov et al., 2004) confirmed these observations and provided the first structural insights into natural RNA aptamers. As predicted, the L2 and L3 form a tertiary interaction with two G-C Watson-Crick pairs at its core (G38-C60 and G37-C61) essential for stable formation of the pseudoknot (Fig. 2b). These pairs are buttressed by a set of non-canonical base pairs that are of lesser importance, but still make significant energetic contributions to the RNA's structure (Gilbert et al., 2007; Lemay et al., 2006). This structural feature places P2 and P3 into a close parallel arrangement, and organizes the RNA into a common architectural theme of a three-way junction supported by a distal tertiary interaction (de la Pena et al., 2009).

Direct ligand recognition by the riboswitch aptamer domain is enabled through formation of a complex binding pocket by the three-way junction (Batey et al., 2004; Serganov et al., 2004). The junction itself is defined through the coaxial stacking of P1 on P3, and formation of a series of base triples between conserved nucleotides. At the heart of this structure is the ligand that as predicted forms a Watson-Crick interaction with the nucleotide 74, and is further recognized through a base triple involving U51 and an additional hydrogen bond between N7 and the 2'-hydroxyl group of U22 (Fig. 2c). This mode of interaction was supported by a concurrent NMR study (Noeske et al., 2005). A single point mutation, C74U, within the *xpt* aptamer causes enables this aptamer to switch its discrimination from guanine to adenine, demonstrating that the pyrimidine residue at position 74 is the primary specificity determinant between the guanine and adenine classes (Gilbert et al., 2006b).

The most striking and unexpected feature of these structures is that the ligand is ~98% solvent inaccessible, which requires coupling of the association of ligand binding and a conformational change in the RNA (Batey et al., 2004). Based upon this observation, we proposed the first mechanistic hypothesis of how riboswitches harness ligand binding to direct the downstream secondary structural switch (Batey et al., 2004; Gilbert et al., 2006b). Immediately adjacent to the purine nucleobase binding pocket, nucleotides from J2/3 (49 and 50, Fig. 2a) form base triples with P1, which in-line probing data indicate are ligand-induced (Mandal et al., 2003). These tertiary interactions stabilize formation of the P1 helix such that its 3'-side cannot be used to form the anti-terminator element (Batey et al., 2004). Thus, ligand binding induces a set of localized tertiary interactions involving the 3'-side of the P1 helix that serves to direct the secondary structural switch. This feature of riboswitches has now been observed in many other structures and is now generally accepted as the primary means by which ligand binding regulates genetic regulation (Haller et al., 2011b).

2.2 The purine riboswitch family: the 2'-deoxyguanosine class

A third class of purine riboswitches has been observed in only a single organism, *Mesoplasma florum*. In this genome eight purine riboswitches were identified, some of which displayed a number of deviations from the guanine/adenine class consensus sequence (Kim et al., 2007). Two of these riboswitches have a strong (>200-fold) selectivity for 2'-deoxyguanosine above guanine or guanosine while two others display marginal

discrimination between these compounds (Kim et al., 2007). The RNA with the highest selectivity for 2'-deoxyguanosine (called “1A”) has a number of nucleotides whose identity deviates from the consensus sequence of the guanine and adenine classes. The terminal loops L2 and L3 differ in both their length and composition, although the core G-C pairs of the L2–L3 interaction are conserved. Within the ligand binding pocket, there were also alterations that involved invariant nucleotides in the guanine/adenine (Kim et al., 2007). Presumably, some of these changes are necessary to adjust the structure of J2/3 to accommodate the 2'-deoxyribosyl moiety that would otherwise occupy the site of U47/U51 observed in the guanine/adenine classes (Fig. 2c).

The basis for discrimination between 2'-deoxyguanosine (2'-dG) and guanine was initially revealed using an approach that systematically converted the *B. subtilis* *xpt* guanine riboswitch into the *M. florum* IA 2'-deoxyguanosine riboswitch (Edwards & Batey, 2009). In this study, changes in the *B. subtilis* riboswitch were first introduced at nucleotides directly involved in ligand binding followed by additional changes moving outward from the pocket. By measuring the binding affinity for each of these RNAs for guanine and 2'-dG, it was revealed that a subset of nucleotides was important for discrimination. In particular, the nucleotide at position 51, which is cytosine in the 2'-dG riboswitches, was shown to be extremely important for switching the specificity of the RNA (Edwards & Batey, 2009). This occurs mostly through a loss of affinity for guanine rather than an increase in affinity for 2'-dG and results in an RNA that has only a small selectivity for 2'-dG (~5-fold). Further changes to the sequence solely around the three-way junction, particularly to base pairs in P2 adjacent to the junction, result in a specific increase in affinity for 2'-dG, leading to a near wild type selectivity for 2'-dG over guanine. Notably, differences in the L2–L3 interaction between the guanine/adenine and 2'-dG classes do not have a substantial impact upon specificity and thus it is likely that only local changes to the structure of the ligand binding pocket are sufficient to confer the selectivity switch (Edwards & Batey, 2009).

Crystal structures of a hybrid *xpt* riboswitch (Edwards & Batey, 2009) and the wild type *M. florum* I-A riboswitch (Pikovskaya et al., 2011) have been solved to provide an atomic level understanding of the above observations. In each RNA, the 2'-dG binding pocket reveals that the crucial C51 is shifted towards C74 to provide room for the 2'-deoxyribosyl moiety and re-establish two hydrogen bonds with the sugar edge of the nucleobase (Fig. 3). While the overall architecture of the junctions is similar, there are small changes observed within the wild type structure that provide further insights into specificity. The most significant difference is that the nucleotide equivalent of A24, which stacks on P3 in the guanine and adenine riboswitches (Fig. 2b), instead forms a base triple with the first base pair of P2 (Pikovskaya et al., 2011). This accounts for the observation that the base pairs at the base of P2 are important for conferring the full specificity switch (Edwards & Batey, 2009). Furthermore, comparison of the *M. florum* IA riboswitch in complex with 2'-deoxyriboguanosine and guanosine revealed that discrimination between the two is likely the result of a destabilization of the binding pocket through a loss of an interaction between the 3'-hydroxy group of the ligand and 2'-hydroxyl group of C56 (the equivalent of position 49 in the *xpt* riboswitch) and a small readjustment of J2/3 (Pikovskaya et al., 2011).

2.3 The preQ₁ riboswitches

The smallest riboswitch aptamer identified to date is one that recognizes an intermediate in the biosynthesis of the hypermodified base queuosine, found at the wobble position of the anticodon in many tRNAs (Roth et al., 2007). Bacteria synthesize this nucleotide starting from GTP, which is transformed into the compounds preQ₀ (7-cyano-7-deazaguanine) and preQ₁ (7-(aminoethyl)-7-deazaguanine) in route to the incorporation of preQ₁ into tRNA and further modification (Vinayak & Pathak, 2010). This sequence element was originally found adjacent to *ykvJ* and *ylbH* genes in a bioinformatic survey for recurring sequence

motifs in bacterial intergenic regions but was considered a poor candidate for a riboswitch (Barrick et al., 2004). Following identification of the *ykvJKLM* operon as involved in queuosine biosynthesis it was demonstrated that the leader sequence of the *Bacillus subtilis queC* gene (renamed from *ykvJ*) binds preQ₁ with ~20 nM affinity (Roth et al., 2007). Related metabolites preQ₀ and guanine bound with moderately lower affinities of ~100 and ~500 nM, respectively (Roth et al., 2007). The low selectivity of the RNA for preQ₁ over preQ₀ and guanine leaves open the possibility of the riboswitch being regulated by these other compounds *in vivo*. A second class of preQ₁ riboswitch has also been identified (preQ₁-II) that shows similar patterns of selectivity (Meyer et al., 2008). While the preQ₁-I class is relatively broadly distributed across Firmicutes, Proteobacteria, and Fusobacteria, the second class is rarely observed outside Streptococcaceae (Meyer et al., 2008).

The preQ₁-I class is further divided into two bioinformatically distinct types that share a similar secondary structure but have a slightly different pattern of nucleotide conservation in the loop (Roth et al., 2007). Each contains a stem-loop structure followed by an adenosine-rich 3' single-stranded region (type II is shown in Fig. 4a, b). Common to both types is a terminal G-C pair in P1, a uridine and cytosine at the 5'- and 3'-ends of L1, and a series of four adenosines in the flanking 3'-tail (green box, Fig. 4a). The primary difference between the two types lies in the conservation pattern of nucleotides that compose the L1/P2 region of the pseudoknot. The relationship of these two types is further emphasized by the fact that certain preQ₁-I riboswitches contain characteristics of both (Meyer et al., 2008). Since essential nucleotides of the preQ₁-I aptamers cluster in a region as small as 33 nucleotides in some phylogenetic representatives, they are the smallest of the validated aptamers (Roth et al., 2007).

Structures of both type I (*T. tengcongensis queT*) (Spitale et al., 2009) and type II (*B. subtilis queC*) (Kang et al., 2009; Klein et al., 2009) aptamers have been recently solved to illustrate how this RNA binds preQ₁ and related metabolites. All three structures, along with an NMR study (Rieder et al., 2009), showed that the aptamer adopts a classic H-type pseudoknot (reviewed in (Staple & Butcher, 2005)) in which nucleotides in a hairpin loop form Watson-Crick base pairing interactions with a 3' single-stranded tail. Unusually, these RNAs have a significant loop (L2) that bulges out between helices P1 and P2 (Fig. 4a, b) (Kang et al., 2009; Klein et al., 2009; Spitale et al., 2009). Other elements of the pseudoknot, on the other hand, reflect standard pseudoknot architecture, including coaxial stacking of the P1 and P2 helices, the extensive use of adenosines in the minor-groove crossing strand (L3) and uridine residues in the major-groove crossing strand (L1). The adenosines of L1 interact with the minor groove face of the Watson-Crick base pairs using a type of "inclined-A" triple in which adenosines are skewed with respect to the helix, allowing it to interact with adjacent base pairs. These types of A-minor triples buttressing a pseudoknot were also observed in the SAM-II (Gilbert et al., 2008) and *glmS* riboswitches (Klein & Ferre-D'Amare, 2006). This is in contrast to the classic type I/II A-minor triples (Doherty et al., 2001; Nissen et al., 2001) which tend to be more in plane with the base pair with which it hydrogen bonds.

Like the purine riboswitch, recognition of the ligand is dominated by formation of a Watson-Crick/sugar edge triple, in this case, with universally conserved cytosine and adenosine residues (Fig. 4c, d). In both types, this triple is augmented by the participation of a uridine with N9 of the nucleobase. In the structure of the type II aptamer (Fig. 4d), the aminoethyl modification interacts with G5 and a nonbridging phosphate oxygen of C12 (Klein et al., 2009). Selectivity for preQ₁ over preQ₀ is presumably achieved through these interactions that are absent in the type I/preQ₀ complex (Fig. 4c). Superimposition of the two structures (PDB ID 3K1V and 3GCA) reveals that the phosphate group of U12 in the type I-Q₀ structure is significantly displaced from the equivalent position (C12) in the type II-Q₁

structure. Thus, the presence of the positively charged amino group in preQ₁ induces a further conformational change around the binding pocket absent in the complex with preQ₀, and presumably the same is true for guanine binding. One interpretation of this is that the difference in conformation may promote formation and/or stabilization of P2, a critical element in the regulatory switch, allowing preQ₁ to be a more effective regulator of this riboswitch. This binding pocket sits at the site of the coaxial stack between P1 and P2 that incorporates other universally conserved nucleotide elements. The most highly conserved of these is a trans Watson-Crick /sugar edge interaction between (G5-C16)•A27 that forms the "floor" of the binding pocket.

Unfortunately, there is currently no structure of a preQ₁-II riboswitch. Like the preQ₁-I class of riboswitches, its central architectural feature is an H-type pseudoknot but with an additional hairpin loop inserted into L3 (Meyer et al., 2008). Notably, the two classes of preQ₁ riboswitches share no common pattern of conserved nucleotides within this pseudoknot motif. The mode of purine recognition is also distinct between the two classes (Meyer et al., 2008). Sequence alignment revealed only one conserved cytosine that is not involved in a base pair; mutation of this residue to a uracil resulted in only a small drop in preQ₁ binding. This suggests that preQ₁-II does not recognize the nucleobase using Watson-Crick pairing unlike the first class (Meyer et al., 2008). Along with S-adenosylmethionine and cyclic-di-GMP riboswitches, this evidence suggests that pre-Q₁ binding RNAs have emerged at least twice in evolution.

2.4 The cyclic-di-GMP riboswitches

Bis-(3'-5')-cyclic dimeric guanosine monophosphate (c-di-GMP) is a second messenger (a compound that relays a signal from a surface receptor to a target inside the cell) that affects many aspects of bacterial physiology and life cycle (reviewed in (Hengge, 2009)). Originally discovered as an effector of cellulose biosynthesis in *Gluconacetobacter xylinus* (Ross et al., 1987), c-di-GMP has been implicated in a number of processes involved in biofilm formation and inhibition of cell motility, control of virulence in pathogens, and cell cycle progression (Hengge, 2009). This compound is produced by diguanylate cyclases that carry a catalytic GGDEF motif and degraded by specific phosphodiesterases to control its intracellular concentrations (Hengge, 2009). Despite its discovery in 1987, the targets of this compound remained elusive for almost twenty years, when the PilZ domain, found as a regulator of a broad array of proteins, was identified as a receptor for c-di-GMP (Amikam & Galperin, 2006; Ryjenkov et al., 2006).

More recently, the Breaker group has identified two classes of riboswitches whose effector is c-di-GMP (Weinberg et al., 2007). The first class, originally coined the "GEMM" (Genes for the Environment, for Membranes, and for Motility) motif, it was found associated with a diverse array of gene functions across both Gram-positive and Gram-negative bacteria. This class is further divided into two types based upon sequence conservation patterns. The first type is defined by the presence of a classic GRRA (R, purine; Y, pyrimidine) tetraloop-tetraloop receptor motif (orange, Fig. 5a) (Weinberg et al., 2007) as exemplified by that found in the P4P6 domain of group I self-splicing introns (Cate et al., 1996; Murphy & Cech, 1994). The second type contains a GYRA-type tetraloop on the first helix and often a receptor motif that is specific for this tetraloop (Weinberg et al., 2007). Analysis of the type I GEMM riboswitch that regulates the *Vibrio cholerae tfoX*-like gene demonstrated a high affinity interaction with c-di-GMP while discriminating against related compounds pGpG and GpG by at least 1000-fold (Sudarsan et al., 2008). Further evidence for other types of GEMM motifs have been cited suggesting an even greater diversity of riboswitches that respond to c-di-GMP (Weinberg et al., 2010). One example is the class II c-di-GMP riboswitch found in *Clostridium difficile* that regulates the splicing activity of a group I intron to regulate gene function (see below) (Lee et al., 2010a).

Several crystal structures of the *tfoX*-like *V. cholerae* type I riboswitch aptamer domain have been recently determined to reveal the atomic-basis for effector recognition (Kulshina et al., 2009; Smith et al., 2009). These structures reveal that the class I c-di-GMP riboswitch, like the purine riboswitch, is centered upon a three-way junction that creates the ligand binding pocket and a distal loop-loop interaction that serves to enforce helical packing (Fig. 5b) (Kulshina et al., 2009; Smith et al., 2009). The GAAA tetraloop forms the same set of interactions with the tetraloop receptor as observed previously, mediated principally by two adenosine minor triples (Cate et al., 1996). A second interaction that promotes helical packing is an isolated C-G (pair formed by C44 and G83 in P2 and P3, respectively) (Fig. 5a, b) (Kulshina et al., 2009; Smith et al., 2009). Notably, the identity of these two nucleotides are amongst the most highly conserved in the class I aptamer and mutation of either one of these nucleotides or conversion to a compensatory U-A pair is highly deleterious to binding (K_{rel} for the C44U/G83A mutation is ~20,000) (Smith et al., 2010). This is greater than disruption of the tetraloop/receptor interaction ($K_{rel} = 1000$) (Smith et al., 2010). The isolated pair is facilitated by an S-turn in the backbone around G83 and a set of base triples (Figure 5b, red) that facilitates underwinding of the P3 helix (Kulshina et al., 2009). Underscoring the importance of this region for riboswitch function, nucleotides involved in this interhelical interaction are >75% conserved in phylogeny.

c-di-GMP is recognized asymmetrically within a binding pocket localized to the three-way junction, mediating coaxial stacking between P1 and P2 (Kulshina et al., 2009; Smith et al., 2009). The first guanine base (G_α) forms a trans Hoogsteen/Watson-Crick base pair with G20 (Fig. 5c), while the second (G_β) forms a Watson-Crick pair with C92 (Fig. 5d). These pairs are buttressed by the ribose sugars of nucleotides 47–49. A highly conserved adenine base (A47) intercalates between the two guanines of c-di-GMP to complete the stacking between P1 and P2. Intriguingly, the bases mediating direct pairing with c-di-GMP are not amongst the most conserved in the aptamer. An adenosine is found 23% of the time at the 20 position and U is found at position 92 in 4% of known sequences, indicating some flexibility in the pairing patterns (Smith et al., 2010). Structures of the G20A and C92U mutants show these nucleotides alter their positions to maintain at least one hydrogen bond in each interaction. The G20A/C92U double mutant binds c-di-AMP with a four-fold greater affinity than c-di-GMP, raising the possibility that there may be riboswitches that respond to this bacterially synthesized molecule (Smith et al., 2009).

While the guanine bases are embedded deeply within the junction, the ribose-phosphate ring is positioned within the major groove (Kulshina et al., 2009; Smith et al., 2009). Interactions with this part of c-di-GMP is mediated in part by a hexahydrated magnesium whose inner sphere coordinated waters hydrogen bond with G19, G20, and the two nonbridging phosphate oxygens of G_α (Smith et al., 2010). The other phosphate moiety apparently does not interact with a metal ion.

The c-di-GMP/class-I riboswitch interaction is the highest affinity small molecule-RNA interaction measured to date (Smith et al., 2009; Sudarsan et al., 2008). Using the electrophoretic mobility shift assay (EMSA) to measure the association/dissociation rates of binding, the apparent equilibrium dissociation constant ($K_{D,app}$) was calculated to be 10 pM (Smith et al., 2009; Smith et al., 2010). The apparent association rate was found to be 1×10^6 M $^{-1}$ sec $^{-1}$, a value comparable to other riboswitches (Zhang et al., 2010). Instead, c-di-GMP has an unusually slow dissociation rate, (1×10^{-5} min $^{-1}$) which corresponds to a half-life of around a month. Despite the exceedingly high affinity these riboswitches have for c-di-GMP, it has been proposed that micromolar concentrations of c-di-GMP are needed to regulate the riboswitch due to the slow approach to equilibrium (see Section 4) (Smith et al., 2009).

A second class of c-di-GMP riboswitch was recently identified as part of an allosterically controlled self-splicing group I intron in *Clostridium difficile* (Lee et al., 2010a). The c-di-GMP binding aptamer is situated immediately upstream of the intron such that when ligand binds the 5' splice site is unmasked and available to form the correct P1 stem for splicing and formation of an mRNA capable of being translated. In addition, like all group I introns, the first step of splicing requires GTP to be bound to a specific site near the 3' end of the ribozyme (reviewed in (Vicens & Cech, 2006)). To properly process this RNA, both compounds must be bound to their respective sites, and thus this represents a case of a ribozyme that requires two inputs to promote expression (Lee et al., 2010a).

The consensus sequence for this second class of c-di-GMP riboswitch suggests a radically different RNA architecture and ligand binding mode from the first class. The secondary structure of this RNA is a stem-loop structure with two internal loop motifs. The first internal loop is a canonical kink-turn (KT) motif that induces a ~60° bend in the RNA (yellow, Fig. 6a) (Goody et al., 2004; Klein et al., 2001). This motif is widely distributed across RNA biology, including the ribosome, snRNAs (Klein et al., 2001), snoRNAs (Moore et al., 2004; Omer et al., 2002), and other riboswitches (Heppell & Lafontaine, 2008; Montange & Batey, 2006; Winkler et al., 2001), and thus represents a fundamental building block in establishing higher-order RNA architecture. A terminal hairpin loop forms a pseudoknot interaction with the other internal loop (cyan, Fig. 6a). Further underscoring the significant differences between the two classes of c-di-GMP riboswitches, a set of conserved nucleotides that would interact with the guanine moieties in the same fashion as in the class I c-di-GMP riboswitches could not be identified (Lee et al., 2010a).

A crystal structure of the *Clostridium acetobutylicum* c-di-GMP riboswitch that controls expression of a carbohydrate binding domain protein was solved to reveal the molecular basis of recognition (Fig. 6b) (Smith et al., 2011). The pseudoknot organizes the RNA such that the binding site for c-di-GMP is at the junction of the P1, P2, and PK helices. This creates a binding pocket in which G_{α} of the ligand participates in formation of an extensive triplex between J2/PK and the pseudoknot (Fig. 6b). G_{β} , on the other hand, forms a single hydrogen bond interaction with a moderately conserved guanosine residue in J2/1 (Fig. 6c). Unlike class I, this RNA almost entirely ignores the ribose-phosphate backbone of the ligand. The only significant commonality between the two classes with respect to c-di-GMP recognition is the insertion of an adenosine between the guanine bases of the ligand (A70, Fig. 6c) (Smith et al., 2011). The class II riboswitch exhibits reduced specificity for c-di-GMP as compared to class I (Shanahan et al., 2011), which could be exploited in the design of compounds that can target one class while leaving the other unaffected (Smith et al., 2011).

2.5 The tetrahydrofolate (THF) riboswitch

The aforementioned riboswitches generally exhibit a very high specificity for their effector over chemically similar compounds that could be found in the cellular environment. However this may not hold true for all riboswitches. An example of such a crossover in specificity was recently revealed in a study of the tetrahydrofolate (THF) riboswitch (Trausch et al., 2011). While tetrahydrofolate (THF) itself is not a purine-bearing compound it contains a pterin moiety that is structurally similar to guanine, differing by the addition of a sixth carbon to the imidazole ring. When the structure of the THF riboswitch was solved it became immediately clear that the similarity of these two compounds could present a challenge to this RNA.

Like the purine and di-cyclic-GMP riboswitches the THF riboswitch uses an architectural motif consisting of a three-way junction supported by a distal tertiary interaction (Ames et al., 2010). In this case (Fig. 7a, b), the P1 regulatory helix is adjacent to the tertiary

interaction, a pseudoknot between L3 and J2/1 (red, Fig. 7b), rather than the junction. The most unusual aspect of this structure was the observation of two distinct ligands in the aptamer domain: one THF site embedded within the three-way junction ($\text{THF}_{3\text{WJ}}$) and a second within the pseudoknot (THF_{PK}) (Trausch et al., 2011). This arrangement has never been observed in another aptamer, synthetic or biological. Chemical probing and single-turnover transcription assays demonstrated that while both sites bind THF with nearly the same affinity the pseudoknot site is much more critical for the regulatory activity of the RNA than the three-way junction site. This is consistent with other riboswitches, which invariably place the ligand-binding site adjacent to sequences elements that are involved in directing the regulatory secondary structural switch. It should be noted that another structural study of the THF riboswitch identified only the three-way junction site (Huang et al., 2011). This is because the RNA has a “domain swap” such that the first nine nucleotides of the RNA are swapped with the same sequence in an adjacent molecule in a crystal lattice. This distorts a critical nucleotide in the THF_{PK} binding pocket to prevent productive ligand binding at this site. Instead, this structure somewhat reflects the “ON” state of the aptamer domain in which the antiterminator has formed at the expense of the P1 helix.

Both ligand binding sites recognize the ligand in a similar fashion (Fig. 7c, d). The primary interactions at each site occur through hydrogen bonding interactions between the reduced pterin moiety and the RNA involving the N1/N8 and N3 faces of the pterin and pyrimidine residues. Note that these interactions are very similar in nature to how the guanine riboswitch interacts with its effector (Fig. 2c). This mode of interaction is consistent with several observations made through a biochemical analysis by the Breaker group (Ames et al., 2010). First, this RNA discriminates against folic acid in favor of its reduced forms, including dihydrofolate and tetrahydrofolate. In large part, this would be due to the loss of a productive hydrogen bond between N8 (numbering shown in Fig 7c) of the reduced pterin and a uridine residue (U7 in $\text{THF}_{3\text{WJ}}$ or U25 in THF_{PK}). Second, this RNA does not appear to discriminate between various derivatives of THF that carry a one carbon unit at N5, consistent with the lack of contacts to this face of the pterin ring. Finally, the RNA does not appear to require either the p-aminobenzoate (pABA) or the glutamyl moieties for high affinity binding, which is reflected by the finding that only the pABA group forms van der Waals interactions with the RNA. Taken together, these data suggested that guanine or closely related derivatives may be capable of productively interacting with the RNA. This was verified by isothermal titration calorimetry, which showed that 7-deazaguanine bind at each site with nearly the same affinity as THF.

However, ligand binding to a riboswitch receptor does not necessarily translate into regulatory activity. Single-turnover transcription assays using 7-deazaguanine and guanine revealed that these compounds regulate the switch with ~100-fold less efficiency than THF. This discrepancy is likely a result of differences in the binding kinetics of THF and guanine (see Section 4). As a result, this riboswitch is responsive to only the reduced folate pool in the cell. However, the intracellular concentration of guanine in rapidly dividing *E. coli* is sufficiently high (~100 μM , (Bennett et al., 2009)) to raise the possibility that guanine could act as a competitive inhibitor of this riboswitch, although the biological rationale for this behavior is not clear.

2.6 Other purine-binding riboswitches

While the above riboswitches are considered part of a purine-binding group of RNAs (with the exception of THF, which is considered to part of the coenzyme binding group), other riboswitches contain ligands that have purine components. The most obvious example is the *S*-adenosylmethionine and *S*-adenosylhomocysteine binding riboswitches that all appear to recognize the effector’s adenosyl moiety (reviewed in (Batey, 2011)). Like most of the purine binding riboswitches, a significant component of each ligand-RNA interaction is

mediated through base pairing or tripling with the adenine base. Another example is the adenosylcobalamin riboswitches, which appear to specifically recognize the 5'-deoxyadenosyl group (Gallo et al., 2008; Nahvi et al., 2002). Finally, a class of riboswitches that recognize the molybdenum/tungsten cofactors (Moco/Tuco) that contain a pterin moiety similar to that of THF riboswitch have been identified (Regulski et al., 2008). Like the THF riboswitch, these RNAs may also bind guanine due to its similarity to pterin. In addition to the above riboswitches, there may be other purine-binding riboswitches that are yet to be discovered. For example it has been noted that if riboswitches are truly ancient biological relics, then one might expect to find nicotinamide dinucleotide (NAD) and CoA binding classes (Breaker, 2011). If these do exist, then it is certain that they are rare and thus difficult to identify. Since it has been estimated that there may be hundreds of rare riboswitches yet to be discovered (Breaker, 2010), it is highly likely that there are many more purine-binding riboswitches that have yet to be characterized.

3. Folding of the purine riboswitch

Efficient acquisition of secondary and tertiary structure is essential for riboswitches to act as effective regulators of gene expression. At least half of the known riboswitches control expression at the transcriptional level (Barrick & Breaker, 2007) and thus obligatorily have a small window of opportunity in which to act before RNA polymerase (RNAP) proceeds past the intrinsic terminator (Garst & Batey, 2009). Slow folding or misfolding of the riboswitch leading to unproductive conformations is potentially extremely problematic. Misfolding of an “OFF” switch for example would disrupt the terminator element allowing for leaky expression in the presence of high concentrations of ligand. Thus there is likely to be substantial evolutionary pressure on the RNA aptamers to rapidly fold with a high probability of reaching the appropriate regulatory state. Because of these considerations it is important to characterize folding events including formation of the ligand-binding aptamer, conformational or folding changes coupled to ligand binding, and folding of the downstream structural switch.

3.1. Single molecule studies reveal a hierarchical pathway of secondary structure acquisition

Ideally, folding of the riboswitch should be experimentally observed as it exits the RNAP during transcription to yield the most biologically relevant folding landscape. Unfortunately, there are only a few insights into this process due to the technical difficulty of such approaches (reviewed in (Pan & Sosnick, 2006; Zemora & Waldsich, 2010)). Instead, studies of RNA folding generally use a fully synthesized aptamer or riboswitch and observe its acquisition of secondary and/or tertiary structure (the principles of RNA folding in vitro is discussed in (Schroeder et al., 2004)). In this experimental approach there is the potential for downstream sequences to interfere with the folding of the 5'-side of the RNA by creating kinetic folding traps or competing secondary structures not available in the biologically relevant folding pathway. The 5'-to-3' polarity of RNA folding and structure acquisition mirroring transcription is most evident in studies of the kinetic assembly of the 30S ribosomal subunit (Shajani et al., 2011), and certainly influences the folding of other large RNAs as well (Pan & Sosnick, 2006).

Insights into secondary and tertiary structure acquisition in riboswitches have been provided by single molecule force extension spectroscopy. In this experimental setup, a transcriptionally stalled RNA molecule is secured at each end by optical traps that can exert a variable force on the molecule; folding or unfolding of the molecule is measured as distance changes between the two traps as a function of force (reviewed in (Neuman & Nagy, 2008; Woodside et al., 2008)). A study of the *B. subtilis pbuE* adenine riboswitch aptamer domain was able to deduce a folding pathway starting from a fully extended RNA

with no secondary or tertiary structure (Greenleaf et al., 2008b). A hierarchical folding pathway was observed in which the P2 and P3 stem-loops fold first (secondary structure acquisition), followed by formation of the L2–L3 interaction (tertiary structure) and an adenine-binding competent state (which, presumably, includes formation of some architectural features of the three-way junction), and finally formation of the P1 helix. In the absence of adenine, the “adenine-competent” state without P1 fully formed is the most populated state, whereas in the presence of adenine the completely folded RNA with P1 formed dominates (Greenleaf et al., 2008b). The observed ligand dependent stabilization of the P1 helix agrees with a model of ligand-induced stabilization of the aptamer domain previously proposed based upon structural and bulk biochemical experiments (Batey et al., 2004; Gilbert et al., 2006b).

A key result of this study was to relate the kinetics of folding, ligand binding, and transcription. The rate of folding was measured to be $k_{fold}=0.4\text{ s}^{-1}$, while the kinetics of adenine binding were measured to be $k_{on}=8 \times 10^4 \text{ M}^{-1} \text{ s}^{-1}$ and $k_{off} = 0.2 \text{ s}^{-1}$ (Greenleaf et al., 2008b). These values suggest that folding and saturation of the aptamer by ligand are on the same timescale as transcription of the aptamer (time constants in the 2–4 second regime for each). Since the *pbuE* expression platform is ~40 nucleotides (nt) long and transcription proceeds at ~40 nt s⁻¹, in the absence of other influences that would act to slow down the polymerase the total time in which the aptamer has to reach equilibrium with the cellular environment is ~1 s. Thus, these data strongly suggest that the kinetics of riboswitches play a significant role in dictating the concentration range of ligand to which they respond in the cell (see Section 4).

A similar set of studies with the *V. vulnificus add* adenine riboswitch that controls translation yielded a similar folding pathway (Neupane et al., 2011). Importantly, these studies were extended to the complete riboswitch, including the downstream expression platform containing the secondary structural switch that represses translation in the absence of adenine. In the presence of adenine, binding of the ligand stabilizes the aptamer, and most critically, the P1 helix and the RNA is locked into the “ON” state. In the absence of ligand, the P1 helix is moderately stable but the aptamer can rapidly fluctuate between the “ON” state and the “OFF” state in which a competing repressing hairpin is formed at the expense of P1. Given the timescales of binding the ribosome these data indicate that the “ON” and “OFF” states are in equilibrium, consistent with the *add* riboswitch being dictated by the thermodynamics of adenine binding (see Section 4) (Neupane et al., 2011). This is consistent with ensemble measurements of the entire *add* riboswitch using 2-AP labeled RNA, which also showed that in the absence of ligand, the *add* riboswitch “ON” and “OFF” states are in equilibrium (Rieder et al., 2007). Interestingly, this study also found evidence for a small population of RNA that misfolds (0.3%) into alternative stem-loop structures, although this off folding pathway may be even less populated in the context of transcription (Neupane et al., 2011).

3.2. A linkage between tertiary structure formation and ligand binding

Another perspective on the folding of the purine riboswitch aptamer is given through single molecule FRET. In contrast to the above folding studies, this experiment starts with the aptamer having fully acquired secondary structure and formation of the L2/L3 tertiary interaction and the three-dimensional organization of the helical elements are observed. In a study of the *B. subtilis pbuE* adenine aptamer, L2 of the aptamer domain was labeled with a fluorescein donor and L3 with a Cy3 acceptor and FRET was observed in single aptamers using total internal reflection microscopy (Lemay et al., 2006). In the absence of magnesium or adenine, the molecules primarily exhibit a low fluorescence state that corresponds to the loops not interacting. At magnesium concentrations around ~20 μM, the RNA interconverts between low, intermediate, and high FRET states with the latter state assigned as having the

L2–L3 interaction formed. Addition of adenine (50 μ M) at very low magnesium concentrations (~2 nM) also elicits this behavior; higher concentrations of adenine and/or magnesium cause the aptamer to become locked in the high FRET state. These data highlight the dynamic nature of the tertiary architecture of the aptamer as well as the relationship between magnesium and ligand in the formation of the “native” structure.

A similar study of the *xpt* guanine riboswitch using fluorophores attached to each of the three helices in pairwise combinations yield similar results (Brenner et al., 2010). By observing all three pairwise combinations, it was possible to observe that the P1/P3 coaxial stack is stable, the P2 helix is highly dynamic and samples two specific orientations relative to P1 and P3, one of which has a transiently formed L2–L3 interaction. Again, addition of a low amount of magnesium (>250 μ M) or guanine locks the aptamer into a rigid state that corresponds to the crystallographically observed state (Brenner et al., 2010).

Time resolved NMR spectroscopy has also been utilized to further study the linkage between ligand binding and tertiary structure formation and stabilization in the *xpt* riboswitch (Buck et al., 2011; Noeske et al., 2007). To be able to observe ligand-induced stabilization of the L2–L3 interaction and the three-way junction, a compound was synthesized in which a photolabile dimethoxy-nitrophen group was linked to the O6 of hypoxanthine (Noeske et al., 2007). Upon light-induced release of hypoxanthine, resonances of the imino protons (protonation of N1 of guanine and N3 of uridine) where followed as a function of time. Kinetic analysis of these signals revealed two distinct kinetic regimes. A “fast” set of half-lives ($t_{1/2} = 18.9 – 23.6$ s) was observed around the three-way junction that was ascribed to an initial docking of the ligand with the RNA. A second set of “slower” kinetics ($t_{1/2} = 27.1 – 30.7$ s) was observed primarily in L2 and P2 and suggesting a subsequent stabilization of the loop-loop interaction and global tertiary architecture (Noeske et al., 2007). Further analysis of these kinetics by use of a destabilizing G37A/C61U mutation (Fig. 2a) revealed that magnesium ions also facilitate this interaction in the absence of ligand (Buck et al., 2011). An independent study by the Varani group on the *add* riboswitch using fast NMR techniques proposes a similar pathway involving an initial adenine docking event followed by a slower set of steps in which the long range L2–L3 is formed (Lee et al., 2010b). In this pathway, formation of the final state, which presumably is that observed in the crystal structure, requires ~3 minutes. Together, both smFRET and NMR point to a synergy between ligand binding and stable acquisition of the global tertiary architecture. This may be an important component of how ligand binding directs downstream folding events to yield the appropriate regulatory response.

3.3. Mechanism of coupling tertiary structural changes to the regulatory response

The crystal structure of the guanine and adenine riboswitch clearly revealed that a local conformational change around the three way junction must be coupled to binding, as the ligand is nearly solvent inaccessible (Fig. 2c). To observe ligand-dependent local folding around the three way junction, a newly developed chemical footprinting technique was applied to the *xpt* guanine riboswitch aptamer (Stoddard et al., 2008). This technique utilizes *N*-methylisatoic acid (NMIA), which specifically reacts with the 2'-hydroxyl groups of RNA to give an adduct that is visualized as a reverse transcriptase stop on a sequencing gel (Merino et al., 2005; Wilkinson et al., 2006). This method, referred to as “SHAPE” (Selective 2'-Hydroxyl Acylation analyzed by Primer Extension), is capable of interrogating every nucleotide position in an RNA, providing specific information about its structure and dynamics (reviewed in (Weeks & Mauger, 2011)). NMIA preferentially reacts with nucleotides whose 2'-hydroxyl can access the C2-*endo* configuration that places the reactive group further away from the non-bridging phosphate oxygen, thereby lowering its local pK_a and increasing its reactivity (Merino et al., 2005). The SHAPE reactivity of a specific nucleotide is correlated to its conformational flexibility. It has been shown that there is a

significant correlation between the NMR S² order parameter and the extent of NMIA reactivity of a nucleotide position (Gherghe et al., 2008). A more recent study correlated SHAPE reactivity to 2-AP fluorescence; the more NMIA reactive sites across three distinct riboswitches were found to be optimal sites for labeling RNA for use in folding and kinetic studies (Souliere et al., 2011). Another advantage to SHAPE chemical probing is that it has been optimized to investigate the thermal unfolding RNA with nucleotide resolution, a significant improvement over traditional optical melting techniques in which is often difficult to assign a transition to a specific region of the RNA of interest (Wilkinson et al., 2005).

Applying this technique to the thermal unfolding of the *xpt* aptamer in the absence and presence of hypoxanthine provided specific insights into how ligand dependent conformational changes can direct gene expression (Stoddard et al., 2008). Analysis of the apparent melting temperature ($T_{m,app}$) for each nucleotide revealed that only a small subset of nucleotides in the aptamer have behaviors that differ in the unbound and bound states (red, Fig. 8). Primarily, these nucleotides are U48–U51 in J2/3 that form one side of the ligand binding pocket. In the absence of hypoxanthine, this region was dynamic at all temperatures, but when ligand was bound, they exhibited a $T_{m,app}$ of ~40 °C. The other nucleotide that shows a large ligand-dependent change in its $T_{m,app}$ is U22 (J1/2); the 2'-hydroxyl group of this nucleotide forms a direct hydrogen bond with the ligand that accounts for this stronger protection over nucleotides in this region of the RNA. Conversely, J3/1 showed no ligand dependence to its melting behavior (grey, Fig. 8). These data implied two things. First, that J2/3 acts as a flexible “lid” that encapsulates the nucleobase after initial encounter with the binding pocket. This conclusion was also reached in a study that used NMR approaches that monitored guanine induced conformational changes in the *xpt* riboswitch (Ottink et al., 2007). The initial docking event between ligand and RNA is most likely mediated through nucleotide 74 that is organized by coaxial stacking of J3/1 (Stoddard et al., 2008). In turn, this preorganization of J3/1 is enforced by formation of L2/L3, as all three elements undergo ligand-independent thermal transitions around 55 – 60 °C. Thus, distal tertiary interactions in the *xpt* riboswitch that form independently of the ligand serve to facilitate partial organization of the binding pocket for ligand recognition. This is unlike the *add* and *pbuE* adenine riboswitches where the formation of the L2–L3 interaction is strongly coupled to ligand binding (see previous section). Second, coupled to the folding of J2/3 around the ligand is formation of base triples between J2/3 and the 3'-side of P1. This suggests that stable incorporation of the P1 helix into the aptamer—versus formation of the competing antiterminator hairpin in the expression platform—is directed by ligand induced tertiary interactions with a sequence element shared between the two domains (Stoddard et al., 2008). This feature of the purine riboswitch has also been found in other families including SAM-I (Stoddard et al., 2010) and FMN (Vicens et al., 2011), and likely reflects a common mechanism for coupling ligand binding to the downstream regulatory secondary structural switch.

3.4. The purine riboswitch on a fast time scale

Yet another perspective on the dynamics of the purine riboswitch is revealed by time-resolved fluorescence spectroscopy. In this method, the fluorescence of a fluorophore incorporated into a macromolecule or complex is monitored as a function of time following excitation by a laser pulse (this technique as applied to RNA is reviewed by Zhou and Xia (Zhao & Xia, 2009)). The fluorescence lifetime of the fluorophore as it relaxes back to its ground state is highly sensitive to its chemical environment. By deconvoluting the decay profile into individual rates information about the dynamics and heterogeneity of the system can be obtained on the picosecond to nanosecond timescale. In various applications of this approach, the fast dynamics of a number of structural features of RNA has been studied,

including stacking interactions of overhanging nucleotides at the 5'- and 3'-ends of RNA (Zhao & Xia, 2007), conformational heterogeneity of the GNRA tetraloop motif (Liu et al., 2008), and the conformational landscape of the HIV transactivation region (Lu et al., 2011).

In one set of studies, the nanosecond dynamics of a 2-aminopurine (2AP)-purine aptamer complex was observed by measuring the fluorescence decay of the 2AP ligand (Eskandari et al., 2007; Prychyna et al., 2009). The observed decay curve was deconvoluted into rates corresponding to the free fluorophore and three 2AP-RNA distinct conformers of a 2AP-aptamer complex. The temperature, magnesium, and RNA concentration dependence of the amplitudes of the individual components of the fluorescence decay curve were used to evaluate the affinity of 2AP and Mg²⁺ for each of these states as well as their thermal stabilities. These data suggested that one of these states corresponds to the crystallographically observed structure, while the two other conformers are different. These other 2AP-bound conformers were proposed to have P2 helix pushed away from the P1/P3 coaxial stack (called the “open” configuration) such that the L2 and L3 do not interact. A comparison of guanine and adenine aptamers suggests that this equilibrium in guanine riboswitches is shifted more towards the “closed” form than either adenine binding variant.

In a more recent study of the *xpt(C74U)*, *pbuE*, and *add* riboswitches Xia and coworkers were able to examine the decay dynamics of 2AP on the picosecond timescale to reveal significant heterogeneity in the binding pocket (Jain et al., 2010). To be able to interpret the nature of the observed decay components, they substituted 7-deazaguanine at the A21, A52, and A73 positions, which acts as a quencher of 2AP fluorescence. From these data, a model of the heterogeneity in the binding pocket was proposed in which the ligand occupies distinct positions that have different stacking interactions with surrounding bases (Fig. 9). Besides a state in which the ligand does not substantially stack with neighboring bases in the RNA—the crystallographically observed state—which dominates the total population, two distinct subpopulations were observed. The first set correlates to increased stacking of the ligand with A21 and/or A51 (thick arrows, Fig. 9) while a second very minor population stacks with U22 or U75 (thin arrows, Fig. 9). These states are all proposed to have low energy barriers between them (1–2 kcal mol⁻¹) and interconvert on the 1–2 nanosecond timescale. The authors make several important points about their observations. First, the conformers described in their model of the heterogeneity of the binding pocket represent its elasticity rather than plasticity. That is, the overall organization of the RNA around the ligand does not appreciably change in this timescale and thus reflects movement of 2AP in a relatively rigid space. Second, they refrain from correlating the states in the binding pocket to changes in the global structure, in contrast to O’Neill and coworkers. Instead they argue based upon a number of other studies that under the conditions used in the ultrafast dynamics measurements, saturating ligand and 2 mM magnesium, all three aptamers are likely predominantly in the global “closed” conformation seen by crystallography.

4. Kinetic versus thermodynamic control

As a consequence of the limited amount of time many riboswitches have to fold, interrogate the cellular environment and potentially bind a small molecule, and form the appropriate secondary structure in the expression platform there can be significant kinetic constraints on its activity. Certainly, all transcriptional riboswitches are constrained by the need to make a decision when the RNAP reaches the intrinsic terminator. Translational regulation may not be similarly constrained, but the pioneering round of translation to transcription in bacteria could complicate the process (Burmann et al., 2010; Proshkin et al., 2010). For example, active translation may be required to prevent rho from prematurely terminating transcription (Peters et al., 2011). In this mechanism, there may be kinetic constraints to productively loading the ribosome and initiating translation. On the other hand, since translational

initiation can occur at any point during the productive lifetime of the mRNA, long after transcription is completed, the riboswitch may have ample time to reach equilibrium and even act as a fully reversible switch.

Studies of two adenine responsive “ON” switches riboswitches (expression of the mRNA is promoted when the effector is bound)--one that controls transcription (*B. subtilis pbuE*) and the other translation (*V. vulnificus add*)--suggest that they indeed differ in their relationship between the aptamer domain and expression platform. In two independent binding studies of the *pbuE* adenine riboswitch the affinity of the RNA for 2AP (Lemay et al., 2006) or adenine (Wickiser et al., 2005a) was compared between the aptamer domain alone and the full length riboswitch. While the aptamer bound each of these compounds with high affinity ($K_{D,app}$ for each is ~500 nM), the full length construct has nearly no affinity for ligand. This indicates that the full length riboswitch is constitutively folded into the “OFF” conformation that disrupts the aptamer in favor of a transcriptional terminator. Conversely, the full length *add* adenine riboswitch can bind adenine nearly as well as the aptamer alone (2300 vs. 680 nM, respectively) (Rieder et al., 2007). This finding implies that this riboswitch is a “bistable” RNA that can reversibly interconvert between the “ON” and “OFF” states with adenine only binding the “OFF” state. A recent detailed comparison of these two riboswitches using approaches that focused upon transcriptional or translational regulation support these conclusions (Lemay et al., 2011).

Based upon the above observations, it was proposed that transcriptional riboswitches are under *kinetic control* while translational riboswitches are under *thermodynamic control* (Rieder et al., 2007; Wickiser et al., 2005a). The most easily observed manifestation of this phenomenon is a difference between the concentration of ligand required to half-saturate the aptamer (K_D) and that required to elicit a half maximal regulatory response (T_{50}) (Wickiser et al., 2005b). To understand the basis for a kinetically controlled process, the association and dissociation rates (k_{on} and k_{off}) of ligand binding to the aptamer must be related to the timescale of transcription between the point when the aptamer is fully transcribed—essentially $t=0$ where the aptamer can begin to equilibrate with a defined intracellular ligand concentration—and when RNAP reaches the regulatory decision point (referred to as t_{tx}). A very simple model of this process assumes (1) that the folding of aptamer is fast such that it can begin to productively bind ligand nearly immediately after the RNAP finishes synthesis of the aptamer domain and (2) secondary structural switching between P1 and the antiterminator helix is fast, both of which are not necessarily good assumptions (see Section 3.1). The time dependence of the approach of the aptamer to equilibrium at a given concentration of ligand (which assumes that the ligand concentration in the cell is static in the timeframe of the response) is given by the relaxation equation

$$\tau^{-1} = k_{obs} = k_{on}([L] + [R]) + k_{off} \quad (1)$$

where k_{obs} is the observed rate of approach to equilibrium, τ is the time constant defined as the time required for the system to reach $1-e^{-1}$ (63.2%) of its progress towards steady-state equilibrium, $[L]$ is the ligand concentration, and $[R]$ is the mRNA concentration. Formation of the RNA-ligand complex as a function of time is

$$[RL]_t = ([RL]_{t=\infty})(1 - \exp(-k_{obs}t)) \quad (2)$$

where t is time and $[RL]$ is the concentration of ligand-RNA complex. At equilibrium ($t = \infty$),

$$[RL]_{t=\infty} = (k_{on}[R][L]) / (k_{on}[L] + k_{off}) \quad (3)$$

Using the above equations and a reasonable estimate of the concentration of a particular mRNA as 1×10^{-12} M the fractional saturation of the aptamer can be determined for a given transcription time ($t = t_{tx}$) as a function of ligand concentration.

Applying the observed association and dissociation kinetics of adenine binding to the *pbuE* aptamer at 35 °C (2.6×10^{-5} M $^{-1}$ s $^{-1}$ and 0.15 s $^{-1}$, respectively (Wickiser et al., 2005a)) reveals how the riboswitch's T_{50} can diverge from the aptamer's K_D (Fig. 10a). As a consequence of equation (1), at low ligand concentration the dissociation constant term dominates the observed rate of approach to equilibrium (k_{obs}). If transcription through the expression platform is sufficiently slow, such that $t_{tx} \gg 1/k_{off}$, then T_{50} converges on the K_D ($1/k_{off}$ is 6.6 s in the example in Fig. 10a). Thus, as t_{tx} increases (the time required for RNAP to transcribe the expression platform), the binding curve approaches the limit of $t = \infty$, representing full equilibration. If the $T_{50} = K_D$, this is defined as thermodynamic control such that the aptamer has sufficient time to fully equilibrate with the cellular environment prior to the regulatory decision. Conversely, at short interrogation times the amount of ligand required to half-saturate the aptamer at the time of the regulatory decision increases, such that $T_{50} > K_D$, which defines kinetic control. This can be clearly seen by replotted the above data as t_{tx} versus the T_{50}/K_D ratio (Fig. 10b). As the typical speed of a bacterial RNAP is 40–50 nt/s and the *pbuE* aptamer is ~25 nucleotides long, in the absence of other influencing factors, $t_{tx} \cong 0.5$ s that clearly places this riboswitch in the kinetic control regime. Note that in the above model the riboswitch is required to fully switch between the two states. In reality, many riboswitch do not achieve this condition (a good example is the *B. subtilis ribD* FMN riboswitch that transitions between 40% to 60% terminated (Wickiser et al., 2005b)) and thus two additional adjustable parameters need to be added to equation 3 to account for this.

Other factors certainly influence this process to further complicate this model. The timeframe of transcription is heavily influenced by the sequence of the mRNA such as “intrinsic pauses”, uridine-rich tracts that cause the polymerase to temporarily stall, and the transcription elongation factor NusA, that increases the time at which the RNAP spends at pause sites (Wickiser et al., 2005b). In the presence of NusA, the T_{50} for the *B. subtilis ribD* FMN riboswitch drops from 500 to 200 nM, reflecting the increase in the t_{tx} (Wickiser et al., 2005b). Another factor that influences the rate of transcription in the cell is the concentration of the NTPs, reflecting the growth and metabolic state of the cell. For example, reduced UTP pools in the *E. coli* have been shown to result in increased transcriptional pausing in the *pyrB1* leader that in turn disfavors formation of an intrinsic transcriptional terminator (reviewed in (Turnbough & Switzer, 2008)). Under low nutrient conditions, the rate of transcription may slow such that the concentration of effector needed to turn off expression of a gene drops as control moves from a kinetic to a thermodynamic regime. Other parameters such as the rate of folding of the aptamer domain into a binding competent state and the rate of secondary structural switching also play role in this process. Very little is known about the timescales of these processes, but it has been suggested that they are roughly on the same timescale as transcription of the expression platform (Greenleaf et al., 2008a). Thus, while the above model begins to provide an explanation for the relationship between intracellular ligand concentration and regulatory activity it does not account for a multitude of intracellular variables that further define the regulatory landscape.

5. Discovery of novel compounds that bind purine riboswitches

It has been proposed that riboswitches represent an important new set of targets for the development of antimicrobial therapeutics (Blount & Breaker, 2006). There are several stated reasons as to why riboswitches are a favorable new avenue for RNA-targeting drugs (Blount & Breaker, 2006). First, as discussed above, the binding of small molecules to the

aptamer is central to their function. Thus, it is reasoned that it should be possible to find chemical and structural analogs of a riboswitch's natural effector that serve as either inhibitors or activators, depending upon the nature regulatory control. In addition, RNA is already a well-validated target of antimicrobial agents; a number of medically important drugs bind key regions of ribosomal RNA to inhibit or alter translation (reviewed in (Thomas & Hergenrother, 2008)). Second, riboswitches control genes essential for either survival or virulence in a number of medically important pathogens such as *Staphylococcus aureus* (Blount & Breaker, 2006). In some bacteria, one class of riboswitch controls multiple operons, providing an opportunity for an antimicrobial agent to affect multiple proteins or metabolic pathways. In *Bacillus anthracis* there are six individual purine riboswitches controlling nine genes involving purine biosynthesis and transport (Mandal et al., 2003; Mandal & Breaker, 2004a). Targeting a combination of these riboswitches could, in principle, result in starving the cell for purine nucleotides thereby slowing or stopping growth. Finally, riboswitches might be targetable by compounds that would not interact with their human protein counterparts. For example, *S*-adenosylmethionine is a critically important metabolite that interacts with a variety of proteins and RNAs (Loenen, 2006). The structure of the most common SAM riboswitch (called SAM-I) revealed that the RNA recognizes this metabolite in a conformation not observed in its complexes with proteins (Montange & Batey, 2006).

The most compelling evidence for riboswitches as viable targets for antimicrobial therapeutics is the discovery that well-established antimetabolites target riboswitches. For example, roseoflavin is an antimicrobial riboflavin analog isolated from *Streptomyces davawensis* that was recently shown to target flavin mononucleotide (FMN) responsive riboswitches in bacteria (Lee et al., 2009; Ott et al., 2009). In addition, the thiamine pyrophosphate (TPP) riboswitch is targeted by the antimicrobial pyrithiamine pyrophosphate (Sudarsan et al., 2005), and the lysine riboswitch is bound by the antimetabolite *S*-(2-aminoethyl)-L-cysteine (AEC) (Blount et al., 2007). In the latter case, the antimicrobial activity is not a direct result of this compound binding a lysine riboswitch, but mutations in this sequence confer resistance by virtue of upregulating lysine biosynthesis thereby competing out the negative effects of AEC (Ataide et al., 2007).

Several studies indicate that a reasonably diverse array of compounds is capable of specifically bind purine riboswitches (Fig. 11). The binding mode of guanine/adenine to the purine riboswitch immediately suggests that pyrimidines can easily fit within the junction without distorting the RNA structure and form a analogous set of hydrogen bonding interactions (Gilbert et al., 2006a). 2,4,6-triaminopyrimidine (Fig. 11a, 5) binds the *V. vulnificus add* adenine riboswitch with only 10-fold lower affinity than adenine (Fig. 11a, 1) (2 μM and 0.2 μM, respectively) and positions itself in the binding pocket in an identical fashion to the six member ring of adenine (Gilbert et al., 2006a).

To discover new compounds capable of binding purine riboswitches, a recent study applied a molecular docking program, DOCK, to the *xpt*(C74U) adenine binding aptamer (Daldrop et al., 2011). The advantage of this approach is that this program has been extensively used to explore protein-ligand interactions and only requires small alterations of the van der Waals and electrostatic energy parameters to apply it to RNA. As a simplification the authors also considered the RNA around the binding pocket to be structurally rigid. The top scoring compounds of this analysis represented a mixture of known binders such as 2,6-diaminopurine and 2,4,5,6-tetraaminopyrimidine (Fig. 11a, 2 and 6) as well as new compounds such as 1,2,4-triazolo-1,2,4-triazole-3,6-diamine and 3-bromo-1,2,4-thiadiazol-5-amine (Fig. 11a, 3 and 4). The ability of these molecules to bind to the riboswitch as well as other novel hits were validated using a combination of ITC and X-ray crystallography (Daldrop et al., 2011). For all of the compounds whose RNA-ligand

complex structure could be determined, the compound orients itself in the binding pocket to maximize hydrogen bonding with the surrounding bases and 2-hydroxyl group. Importantly, this study lays the foundation for the application of computational approaches to the discovery of small molecules that specifically bind an RNA target. (Daldrop et al., 2011).

While the above study was able to find compounds that dock to a rigid binding pocket, this assumption is not necessarily true. In a survey of guanine and adenine analogs that differ at the 2- and/or 6-positions binding to the *xpt* or *xpt*(C74U) aptamers it was found that the binding pocket exhibits adaptive binding behavior (Gilbert et al., 2009). This was observed in several distinct ways. First, the binding pocket can stabilize an unfavorable tautomer of xanthine (Fig 11b, **9**) to promote additional hydrogen bonding interactions. In this case the RNA stabilizes the enol form of xanthine, allowing for formation of two additional productive hydrogen bonds between the ligand and U51/C74. The second means of adaptive binding is through the ability of the nucleotide at position 74 to form a minor groove wobble with the ligand. For example, the adenine analog 2-aminopurine might be expected to be unable to bind to the guanine riboswitch from inspection of the crystal structure. However, biochemical data suggested otherwise; fluorescence measurements of 2AP (Fig. 11c, **(13)**) binding to the *xpt* riboswitch indicates the RNA has only ~10-fold less affinity for this compound than the *pbuE* adenine riboswitch (Lemay & Lafontaine, 2007). The crystal structure of the *xpt*-2AP complex revealed that C74 is shifted towards the minor groove in order to establish two hydrogen bonds between the ligand and nucleotide 74. This behavior was also observed for 6-*O*-methylguanine (Fig. 11c, **(14)**) bound to the *xpt* riboswitch (Gilbert et al., 2009). Yet another compound, 6-chloroguanine (Fig. 11c, **(15)**), can bind the *xpt* and *xpt*(C74U) with almost equal affinity (Gilbert et al., 2009), in part through its ability to exploit halogen bonding (Auffinger et al., 2004; Voth et al., 2007). Together, these data further illustrate how the binding pocket adapts to bind ligands in a way that maximizes hydrogen bonding.

Plasticity of the purine binding pocket was further highlighted by another study that explored the ability of 2- and 6-position substituted guanine analogs to act as antimicrobial agents (Kim et al., 2009). Examination of the crystal structure of the guanine-*xpt* structure suggested to the authors that there might be sufficient space adjacent to the 2- and 6-positions of guanine to accommodate addition of chemical groups while not substantially affecting binding. Somewhat surprisingly, they found that compounds modified with bulky functional groups at these positions bound the RNA with only moderately lower affinity (5 to 10-fold) than guanine. One of these compounds, 2-amino-6-hydroxyaminopurine (Fig. 11b, **(11)**), was shown to both inhibit growth of *B. subtilis* and repress expression of a reporter gene controlled by a guanine riboswitch. However, efforts to find mutants that confer resistance to this compound failed, in part due to its insolubility, leaving its specific mechanism of action an open question (Kim et al., 2009).

Discovery of compounds that productively bind the riboswitch to negatively impact microbial physiology is not necessarily a straightforward exercise in identifying high affinity binders to a target aptamer. An example of this is set forth in a study by Malouin and Lafontaine (Mulhbacher et al., 2010). In light of a study identifying pyrimidine compounds that can productively bind adenine-responsive riboswitches (Gilbert et al., 2006a), they found two pyrimidine compounds that can bind guanine riboswitch aptamers (Mulhbacher et al., 2010). These compounds bind a guanine riboswitch aptamer with ~100 nM affinity (as compared to ~5 nM for guanine), induce a similar set of structural changes as the natural effector, and repress expression of a *lacZ* reporter gene placed downstream of a guanine riboswitch *in vivo* (Mulhbacher et al., 2010). Importantly, they provided strong evidence that one of these compounds, 2,5,6-triaminopyrimidin-4-one (Fig. 11c, **(12)**), was able to block growth of *S. aureus* in a murine model. However, this compound lacked a similar

effect on other microbes that contain guanine riboswitches. They proposed that the effectiveness of this compound in *S. aureus* is due to specific repression of the *guaA* gene (GMP synthetase) rather than broad repression of all genes under control of a guanine riboswitch. Furthermore, 2,5,6-triaminopyrimidin-4-one is only effective in organisms in which it cannot be ribosylated. While the data presented provides compelling evidence this compound is effective at inhibiting *S. aureus* growth in mice, the inability to raise bacteria that contain resistance mutations within the riboswitch suggests that its primary target might be something other than the proposed riboswitch. Nonetheless, this work points the way towards the development of effective new therapeutics that act by targeting riboswitches.

6. Development of new regulatory devices from the purine riboswitch

It is being increasingly recognized that RNA-based devices can fulfill important roles in synthetic biology (Carothers et al., 2010; Isaacs & Collins, 2005; Isaacs et al., 2006). An excellent example of the potential of these devices is an atrazine sensor created by the Gallivan group (Sinha et al., 2010b). Atrazine is a common agricultural herbicide and environmental pollutant associated with birth defects and cancer (Sinha et al., 2010b). In a two-step selection process (Sinha et al., 2011), they first raised an aptamer that specifically binds atrazine followed by a second selection for an expression platform that would enable the aptamer to expose a ribosome binding site in the presence of the ligand thereby creating an “ON” switch. This artificial riboswitch when placed in the leader sequence of an mRNA encoding *cheZ*, a motility gene in *E. coli*, resulted in a bacterium that migrates up an atrazine concentration gradient. Thus, these engineered bacteria have the ability to seek and destroy atrazine in the environment, guided by RNA. However, many RNA-based devices suffer from issues that limit their real world utility (Silverman, 2003; Sinha et al., 2010a).

Natural riboswitches may provide a foundation upon which more robust and easily engineered sensors can be made. To explore this idea Micklefield and coworkers sought variants of the *add* adenine riboswitch capable of responding to nonnatural ligands. To find such RNAs they fully mutagenized the U47 and U51 positions and individually screened each of the 16 mutants for those that could activate chloramphenicol resistance in the presence of a select molecule (Dixon et al., 2010). Screening each mutant against a library of ~80 purine analogs and heterocycles yielded a compound (ammeline or 4,6-diamino-2-hydroxy-1,3,5 triazine) that activates the U47C/U51C and U47C/U51C/U74C variants, which it binds with reasonably high affinity (~1 μM). A crystal structure of the U47C/U51C/U74C variant bound to the related compound azacytosine (Fig. 12) revealed that C51 shifts towards nucleotide 74 in an identical fashion as observed in the 2'-deoxyguanosine binding riboswitch (Edwards & Batey, 2009; Pikovskaya et al., 2011) to maximize hydrogen bonding with the ligand. Most importantly, when these new riboswitches were placed upstream of eGFP in *E. coli*, significant induction of the reporter was observed (Dixon et al., 2010). This study points the way towards engineering novel and practical riboswitches by altering the ligand binding pocket while preserving other features of the RNA such as tertiary architecture and the regulatory switch.

7. Final perspectives

The impact of structural and biophysical approaches in our understanding of riboswitches has been enormous. In large part this was driven by the highly successful efforts to solve the three-dimensional structures of aptamer domains in complex with their effectors. As of this writing, almost every major class of riboswitch has some structural information associated with it. Importantly, from these structures a number of general themes and principles emerge. These RNAs use the same architectural principles such as parallel helical packing (reviewed in detail in (Holbrook, 2008)) and structural motifs like kink-turns and tetraloop-

tetraloop receptor interactions (the use of modular building blocks in RNA structure is excellently reviewed in (Leontis et al., 2006)) as other biological RNAs. Commonalities also exist with respect to ligand recognition. For example, RNAs interacting with purine moieties almost always utilize a pyrimidine-rich pocket to recognize two of the three faces of the nucleobase (Watson-Crick, Hoogsteen, and/or sugar edge). The effector binding site is almost invariably localized within a junction (e.g., purine and class-I c-di-GMP receptors) or pseudoknot (e.g., preQ₁ and THF receptors). These regions afford the RNA the freedom to create the unique architecture necessary to form a pocket that has exquisite shape and chemical complementarity to the ligand. To couple structure and function, these binding sites are always localized adjacent to the critical regulatory switch, generally involving the “P1” helix. Finally, these binding sites often involve extensive burial of the effector molecule, implying a coupling of binding and conformational changes in the RNA.

This last commonality is central to a regulatory mechanism in which global and local ligand-induced conformation changes in the aptamer domain stabilize incorporation of a sequence element into the aptamer that otherwise is used to form one of the secondary structures of the expression platform. Fully understanding the nature of coupling of binding and the switch requires greater insights into the structure of the unbound aptamer, the state that is actively interrogating the cellular environment for the effector. While a number of apo-aptamer structures have been published recently (Garst et al., 2008; Huang et al., 2010; Jenkins et al., 2011; Stoddard et al., 2010; Vicens et al., 2011), most of these structures are extremely “bound-like”. Since a growing crystalline lattice can select out minor conformations from solution, the observed structures may only be rarely sampled in solution. Thus, while these models can be informative (reviewed in (Liberman & Wedekind, 2011)), it is clear that methodologies that provide an ensemble view of the RNA will generate a more accurate perspective of the solution structure of the unbound aptamer. Combinations of NMR, smFRET, and small-angle X-ray scattering (SAXS) approaches have begun to illuminate the dynamic aspects of riboswitch aptamer domains in the absence of their cognate ligand and its relationship to binding (Eichhorn et al., 2011; Haller et al., 2011a; Stoddard et al., 2010). These studies suggest that aptamer domains utilize a “conformational selection” (reviewed in (Boehr et al., 2009; Boehr & Wright, 2008)) mechanism in which the effector binds to conformers in the ensemble that are close in structure to the ligand bound state. Understanding the dynamic ensemble of conformations of the unliganded aptamer may also be a robust route to the discovery of small molecules that target riboswitches (Stelzer et al., 2011).

To clearly define the regulatory mechanism of riboswitches will also require a better description of their kinetic folding landscape in the context of transcription. The inability of full length transcripts to accurately recapitulate biologically relevant folding pathways was highlighted by a study of a small model RNA system that either folds into a single hairpin or branched structure (Xayaphoummine et al., 2007). Strikingly, how the two structures are populated is strongly dependent upon the transcriptional process. This implies that the RNA accesses nonequilibrium structures through cotranscriptional folding that it otherwise may not be able to adopt; this was originally proposed in studies of the thermal unfolding of tRNA^{fMet} (Crothers et al., 1974). Another study by Fedor and coworkers showed that secondary structural exchange in the cellular environment has different energetic landscape than that in vitro (Mahen et al., 2010). In the cell, secondary structural elements can rapidly interconvert with low energy barriers between different conformations, a pathway that may not be possible in vitro. This raises the possibility that biophysical studies alone may never ever really be able to yield a biologically relevant model of the decision making process of riboswitches.

In this light, the most significant challenge moving forward is to directly correlate the increasingly comprehensive structural and biophysical description of purine riboswitch aptamers with their biological activity. The primary impediment is that there is not a robust model system for any purine riboswitch that marries biophysical and biochemical studies with *in vivo* activity, although progress is being made (Lemay et al., 2011). The need for this correlation is motivated by the observation that there are certain aspects of riboswitch behavior only revealed by analysis of their activity in a cellular context. A recent study by Henkin and coworkers demonstrated that the multiple SAM-I riboswitches in *B. subtilis* are “tuned” to meet the regulatory requirements of the operons that they control (Tomsic et al., 2008). Riboswitches that control biosynthetic genes appear to be elicit their SAM-dependent regulatory response at significantly lower concentrations of SAM than those found upstream of transport genes. A range of affinities was also observed for isolated purine riboswitch aptamers, although a correlation to gene function was not noted (Mulhbacher & Lafontaine, 2007). Developing a clearer relationship between the *in vitro* and intracellular behavior of riboswitches will be critical for translating our understanding of these RNAs into practical advances such as the design of new antimicrobial agents or novel biosensors for synthetic biology.

Acknowledgments

The author is grateful to all of the members of his laboratory, past and present, who have made contributions towards our endeavors to understand the structure and mechanism of riboswitches. This work was supported by a grant from the National Institutes of Health (GM073850).

References

- Ames TD, Rodionov DA, Weinberg Z, Breaker RR. A eubacterial riboswitch class that senses the coenzyme tetrahydrofolate. *Chemistry & biology*. 2010; 17(7):681–685. [PubMed: 20659680]
- Amikam D, Galperin MY. PilZ domain is part of the bacterial c-di-GMP binding protein. *Bioinformatics*. 2006; 22(1):3–6. [PubMed: 16249258]
- Ataide SF, Wilson SN, Dang S, Rogers TE, Roy B, Banerjee R, Henkin TM, Ibba M. Mechanisms of resistance to an amino acid antibiotic that targets translation. *ACS chemical biology*. 2007; 2(12): 819–827. [PubMed: 18154269]
- Auffinger P, Hays FA, Westhof E, Ho PS. Halogen bonds in biological molecules. *Proceedings of the National Academy of Sciences of the United States of America*. 2004; 101(48):16789–16794. [PubMed: 15557000]
- Barrangou R, Fremaux C, Deveau H, Richards M, Boyaval P, Moineau S, Romero DA, Horvath P. CRISPR provides acquired resistance against viruses in prokaryotes. *Science*. 2007; 315(5819): 1709–1712. [PubMed: 17379808]
- Barrick JE, Breaker RR. The distributions, mechanisms, and structures of metabolite-binding riboswitches. *Genome biology*. 2007; 8(11):R239. [PubMed: 17997835]
- Barrick JE, Corbino KA, Winkler WC, Nahvi A, Mandal M, Collins J, Lee M, Roth A, Sudarsan N, Jona I, Wickiser JK, Breaker RR. New RNA motifs suggest an expanded scope for riboswitches in bacterial genetic control. *Proceedings of the National Academy of Sciences of the United States of America*. 2004; 101(17):6421–6426. [PubMed: 15096624]
- Batey RT. Recognition of Sadenosylmethionine by riboswitches. *Wiley Interdisciplinary Reviews: RNA*. 2011; 2(2):299–311. [PubMed: 21957011]
- Batey RT, Gilbert SD, Montange RK. Structure of a natural guanine-responsive riboswitch complexed with the metabolite hypoxanthine. *Nature*. 2004; 432(7015):411–415. [PubMed: 15549109]
- Benner SA, Ellington AD, Tauer A. Modern metabolism as a palimpsest of the RNA world. *Proceedings of the National Academy of Sciences of the United States of America*. 1989; 86(18): 7054–7058. [PubMed: 2476811]

- Bennett BD, Kimball EH, Gao M, Osterhout R, Van Dien SJ, Rabinowitz JD. Absolute metabolite concentrations and implied enzyme active site occupancy in *Escherichia coli*. *Nature chemical biology*. 2009; 5(8):593–599.
- Blaxter M. Genetics. Revealing the dark matter of the genome. *Science*. 2010; 330(6012):1758–1759. [PubMed: 21177977]
- Blouin S, Mulhbacher J, Penedo JC, Lafontaine DA. Riboswitches: ancient and promising genetic regulators. *Chembiochem : a European journal of chemical biology*. 2009; 10(3):400–416. [PubMed: 19101979]
- Blount KF, Breaker RR. Riboswitches as antibacterial drug targets. *Nature biotechnology*. 2006; 24(12):1558–1564.
- Blount KF, Wang JX, Lim J, Sudarsan N, Breaker RR. Antibacterial lysine analogs that target lysine riboswitches. *Nature chemical biology*. 2007; 3(1):44–49.
- Boehr DD, Nussinov R, Wright PE. The role of dynamic conformational ensembles in biomolecular recognition. *Nature chemical biology*. 2009; 5(11):789–796.
- Boehr DD, Wright PE. Biochemistry. How do proteins interact? *Science*. 2008; 320(5882):1429–1430. [PubMed: 18556537]
- Breaker RR. Riboswitches and the RNA World. *Cold Spring Harbor perspectives in biology*. 2010
- Breaker RR. Prospects for riboswitch discovery and analysis. *Molecular cell*. 2011; 43(6):867–879. [PubMed: 21925376]
- Brenner MD, Scanlan MS, Nahas MK, Ha T, Silverman SK. Multivector fluorescence analysis of the xpt guanine riboswitch aptamer domain and the conformational role of guanine. *Biochemistry*. 2010; 49(8):1596–1605. [PubMed: 20108980]
- Buck J, Wacker A, Warkentin E, Wohner J, Wirmer-Bartoschek J, Schwalbe H. Influence of ground-state structure and Mg²⁺ binding on folding kinetics of the guanine-sensing riboswitch aptamer domain. *Nucleic acids research*. 2011
- Burmann BM, Schweimer K, Luo X, Wahl MC, Stitt BL, Gottesman ME, Rosch P. A NusE:NusG complex links transcription and translation. *Science*. 2010; 328(5977):501–504. [PubMed: 20413501]
- Carothers JM, Goler JA, Kapoor Y, Lara L, Keasling JD. Selecting RNA aptamers for synthetic biology: investigating magnesium dependence and predicting binding affinity. *Nucleic acids research*. 2010; 38(8):2736–2747. [PubMed: 20159999]
- Carothers JM, Oestreich SC, Davis JH, Szostak JW. Informational complexity and functional activity of RNA structures. *Journal of the American Chemical Society*. 2004; 126(16):5130–5137. [PubMed: 15099096]
- Cate JH, Gooding AR, Podell E, Zhou K, Golden BL, Kundrot CE, Cech TR, Doudna JA. Crystal structure of a group I ribozyme domain: principles of RNA packing. *Science*. 1996; 273(5282): 1678–1685. [PubMed: 8781224]
- Christiansen LC, Schou S, Nygaard P, Saxild HH. Xanthine metabolism in *Bacillus subtilis*: characterization of the xpt-pbuX operon and evidence for purine- and nitrogen-controlled expression of genes involved in xanthine salvage and catabolism. *Journal of bacteriology*. 1997; 179(8):2540–2550. [PubMed: 9098051]
- Couzin J. Breakthrough of the year. Small RNAs make big splash. *Science*. 2002; 298(5602):2296–2297. [PubMed: 12493875]
- Crothers DM, Cole PE, Hilbers CW, Shulman RG. The molecular mechanism of thermal unfolding of *Escherichia coli* formylmethionine transfer RNA. *Journal of molecular biology*. 1974; 87(1):63–88. [PubMed: 4610153]
- Daldrop P, Reyes FE, Robinson DA, Hammond CM, Lilley DM, Batey RT, Brenk R. Novel ligands for a purine riboswitch discovered by RNA-ligand docking. *Chemistry & biology*. 2011; 18(3): 324–335. [PubMed: 21439477]
- De la Pena M, Dufour D, Gallego J. Three-way RNA junctions with remote tertiary contacts: a recurrent and highly versatile fold. *RNA*. 2009; 15(11):1949–1964. [PubMed: 19741022]
- Deveau H, Garneau JE, Moineau S. CRISPR/Cas system and its role in phage-bacteria interactions. *Annual review of microbiology*. 2010; 64:475–493.

- Dixon N, Duncan JN, Geerlings T, Dunstan MS, McCarthy JE, Leys D, Micklefield J. Reengineering orthogonally selective riboswitches. *Proceedings of the National Academy of Sciences of the United States of America.* 2010; 107(7):2830–2835. [PubMed: 20133756]
- Doherty EA, Batey RT, Masquida B, Doudna JA. A universal mode of helix packing in RNA. *Nature structural biology.* 2001; 8(4):339–343.
- Edwards AL, Batey RT. A structural basis for the recognition of 2'-deoxyguanosine by the purine riboswitch. *Journal of molecular biology.* 2009; 385(3):938–948. [PubMed: 19007790]
- Eichhorn CD, Feng J, Suddala KC, Walter NG, Brooks CL 3Rd, Al-Hashimi HM. Unraveling the structural complexity in a single-stranded RNA tail: implications for efficient ligand binding in the prequeuosine riboswitch. *Nucleic acids research.* 2011
- Eskandari S, Prychyna O, Leung J, Avdic D, O'Neill MA. Ligand-directed dynamics of adenine riboswitch conformers. *Journal of the American Chemical Society.* 2007; 129(37):11308–11309. [PubMed: 17713907]
- Gallo S, Oberhuber M, Sigel RK, Krautler B. The corrin moiety of coenzyme B12 is the determinant for switching the btuB riboswitch of *E. coli*. *Chembiochem : a European journal of chemical biology.* 2008; 9(9):1408–1414. [PubMed: 18506875]
- Garst AD, Batey RT. A switch in time: detailing the life of a riboswitch. *Biochimica et biophysica acta.* 2009; 1789(9–10):584–591. [PubMed: 19595806]
- Garst AD, Heroux A, Rambo RP, Batey RT. Crystal structure of the lysine riboswitch regulatory mRNA element. *The Journal of biological chemistry.* 2008; 283(33):22347–22351. [PubMed: 18593706]
- Gherghe CM, Shajani Z, Wilkinson KA, Varani G, Weeks KM. Strong correlation between SHAPE chemistry and the generalized NMR order parameter (S^2) in RNA. *Journal of the American Chemical Society.* 2008; 130(37):12244–12245. [PubMed: 18710236]
- Ghildiyal M, Zamore PD. Small silencing RNAs: an expanding universe. *Nature reviews. Genetics.* 2009; 10(2):94–108. [PubMed: 19148191]
- Gilbert SD, Love CE, Edwards AL, Batey RT. Mutational analysis of the purine riboswitch aptamer domain. *Biochemistry.* 2007; 46(46):13297–13309. [PubMed: 17960911]
- Gilbert SD, Mediatore SJ, Batey RT. Modified pyrimidines specifically bind the purine riboswitch. *Journal of the American Chemical Society.* 2006a; 128(44):14214–14215. [PubMed: 17076468]
- Gilbert SD, Rambo RP, Van Tyne D, Batey RT. Structure of the SAM-II riboswitch bound to S-adenosylmethionine. *Nature structural & molecular biology.* 2008; 15(2):177–182.
- Gilbert SD, Reyes FE, Edwards AL, Batey RT. Adaptive ligand binding by the purine riboswitch in the recognition of guanine and adenine analogs. *Structure.* 2009; 17(6):857–868. [PubMed: 19523903]
- Gilbert SD, Stoddard CD, Wise SJ, Batey RT. Thermodynamic and kinetic characterization of ligand binding to the purine riboswitch aptamer domain. *Journal of molecular biology.* 2006b; 359(3): 754–768. [PubMed: 16650860]
- Goody TA, Melcher SE, Norman DG, Lilley DM. The kink-turn motif in RNA is dimorphic, and metal ion-dependent. *RNA.* 2004; 10(2):254–264. [PubMed: 14730024]
- Greenleaf W, Frieda K, Foster D, Woodside M, Block S. Direct observation of hierarchical folding in single riboswitch aptamers. *Science.* 2008a; 319(5863):630. [PubMed: 18174398]
- Greenleaf WJ, Frieda KL, Foster DA, Woodside MT, Block SM. Direct observation of hierarchical folding in single riboswitch aptamers. *Science.* 2008b; 319(5863):630–633. [PubMed: 18174398]
- Gripenland J, Netterling S, Loh E, Tiensuu T, Toledo-Arana A, Johansson J. RNAs: regulators of bacterial virulence. *Nature reviews. Microbiology.* 2010; 8(12):857–866. [PubMed: 21079634]
- Haller A, Rieder U, Aigner M, Blanchard SC, Micura R. Conformational capture of the SAM-II riboswitch. *Nature chemical biology.* 2011a; 7(6):393–400.
- Haller A, Souliere MF, Micura R. The Dynamic Nature of RNA as Key to Understanding Riboswitch Mechanisms. *Accounts of chemical research.* 2011b
- Hengge R. Principles of c-di-GMP signalling in bacteria. *Nature reviews. Microbiology.* 2009; 7(4): 263–273. [PubMed: 19287449]

- Heppell B, Lafontaine DA. Folding of the SAM aptamer is determined by the formation of a K-turn-dependent pseudoknot. *Biochemistry*. 2008; 47(6):1490–1499. [PubMed: 18205390]
- Holbrook SR. Structural principles from large RNAs. *Annual review of biophysics*. 2008; 37:445–464.
- Huang L, Ishibe-Murakami S, Patel DJ, Serganov A. Long-range pseudoknot interactions dictate the regulatory response in the tetrahydrofolate riboswitch. *Proceedings of the National Academy of Sciences of the United States of America*. 2011
- Huang L, Serganov A, Patel DJ. Structural insights into ligand recognition by a sensing domain of the cooperative glycine riboswitch. *Molecular cell*. 2010; 40(5):774–786. [PubMed: 21145485]
- Huang Z, Szostak JW. Evolution of aptamers with a new specificity and new secondary structures from an ATP aptamer. *RNA*. 2003; 9(12):1456–1463. [PubMed: 14624002]
- Isaacs FJ, Collins JJ. Plug-and-play with RNA. *Nature biotechnology*. 2005; 23(3):306–307.
- Isaacs FJ, Dwyer DJ, Collins JJ. RNA synthetic biology. *Nature biotechnology*. 2006; 24(5):545–554.
- Jain N, Zhao L, Liu JD, Xia T. Heterogeneity and dynamics of the ligand recognition mode in purine-sensing riboswitches. *Biochemistry*. 2010; 49(17):3703–3714. [PubMed: 20345178]
- Jenkins JL, Krucinska J, Mccarty RM, Bandarian V, Wedekind JE. Comparison of a preQ1 riboswitch aptamer in metabolite-bound and free states with implications for gene regulation. *The Journal of biological chemistry*. 2011; 286(28):24626–24637. [PubMed: 21592962]
- Johansen LE, Nygaard P, Lassen C, Agerso Y, Saxild HH. Definition of a second *Bacillus subtilis* pur regulon comprising the pur and xpt-pbuX operons plus pbuG, nupG (yxjA), and pbuE (ydhL). *Journal of bacteriology*. 2003; 185(17):5200–5209. [PubMed: 12923093]
- Kang M, Peterson R, Feigon J. Structural Insights into riboswitch control of the biosynthesis of queuosine, a modified nucleotide found in the anticodon of tRNA. *Molecular cell*. 2009; 33(6):784–790. [PubMed: 19285444]
- Kim JN, Blount KF, Puskarz I, Lim J, Link KH, Breaker RR. Design and antimicrobial action of purine analogues that bind Guanine riboswitches. *ACS chemical biology*. 2009; 4(11):915–927. [PubMed: 19739679]
- Kim JN, Roth A, Breaker RR. Guanine riboswitch variants from *Mesoplasma florum* selectively recognize 2'-deoxyguanosine. *Proceedings of the National Academy of Sciences of the United States of America*. 2007; 104(41):16092–16097. [PubMed: 17911257]
- Klein DJ, Edwards TE, Ferre-D'Amare AR. Cocrystal structure of a class I preQ1 riboswitch reveals a pseudoknot recognizing an essential hypermodified nucleobase. *Nature structural & molecular biology*. 2009; 16(3):343–344.
- Klein DJ, Ferre-D'Amare AR. Structural basis of glmS ribozyme activation by glucosamine-6-phosphate. *Science*. 2006; 313(5794):1752–1756. [PubMed: 16990543]
- Klein DJ, Schmeing TM, Moore PB, Steitz TA. The kink-turn: a new RNA secondary structure motif. *The EMBO journal*. 2001; 20(15):4214–4221. [PubMed: 11483524]
- Kulshina N, Baird NJ, Ferre-D'Amare AR. Recognition of the bacterial second messenger cyclic diguanylate by its cognate riboswitch. *Nature structural & molecular biology*. 2009; 16(12):1212–1217.
- Kuroda MI, Henner D, Yanofsky C. cis-acting sites in the transcript of the *Bacillus subtilis* trp operon regulate expression of the operon. *Journal of bacteriology*. 1988; 170(7):3080–3088. [PubMed: 3133360]
- Lee ER, Baker JL, Weinberg Z, Sudarsan N, Breaker RR. An allosteric self-splicing ribozyme triggered by a bacterial second messenger. *Science*. 2010a; 329(5993):845–848. [PubMed: 20705859]
- Lee ER, Blount KF, Breaker RR. Roseoflavin is a natural antibacterial compound that binds to FMN riboswitches and regulates gene expression. *RNA biology*. 2009; 6(2):187–194. [PubMed: 19246992]
- Lee MK, Gal M, Frydman L, Varani G. Real-time multidimensional NMR follows RNA folding with second resolution. *Proceedings of the National Academy of Sciences of the United States of America*. 2010b; 107(20):9192–9197. [PubMed: 20439766]
- Lemay JF, Desnoyers G, Blouin S, Heppell B, Bastet L, St-Pierre P, Masse E, Lafontaine DA. Comparative study between transcriptionally- and translationally-acting adenine riboswitches

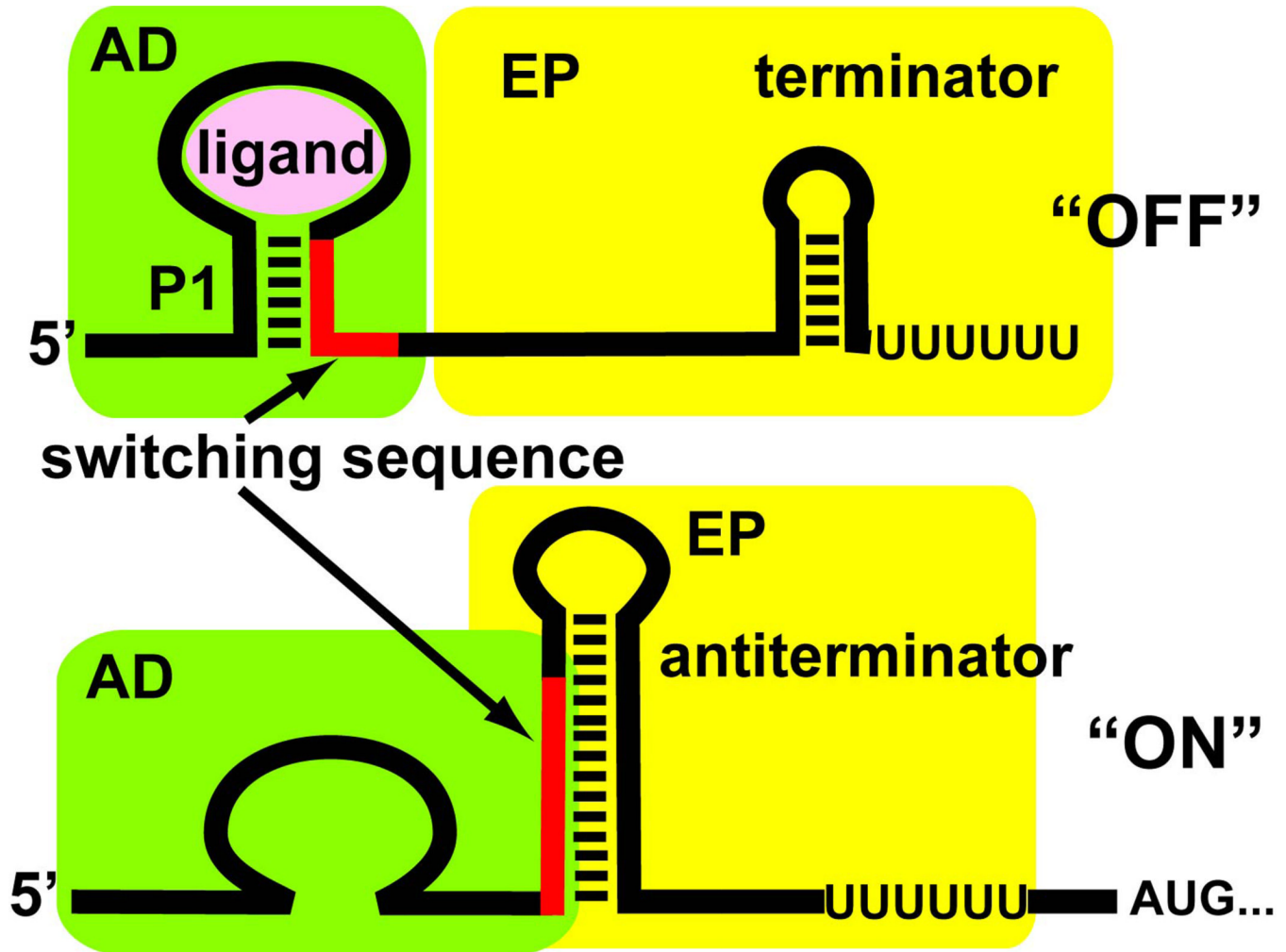
- reveals key differences in riboswitch regulatory mechanisms. *PLoS genetics.* 2011; 7(1):e1001278. [PubMed: 21283784]
- Lemay JF, Lafontaine DA. Core requirements of the adenine riboswitch aptamer for ligand binding. *RNA.* 2007; 13(3):339–350. [PubMed: 17200422]
- Lemay JF, Penedo JC, Tremblay R, Lilley DM, Lafontaine DA. Folding of the adenine riboswitch. *Chemistry & biology.* 2006; 13(8):857–868. [PubMed: 16931335]
- Leontis NB, Lescoute A, Westhof E. The building blocks and motifs of RNA architecture. *Current opinion in structural biology.* 2006; 16(3):279–287. [PubMed: 16713707]
- Leontis NB, Westhof E. Conserved geometrical base-pairing patterns in RNA. *Quarterly reviews of biophysics.* 1998; 31(4):399–455. [PubMed: 10709244]
- Leontis NB, Westhof E. Geometric nomenclature and classification of RNA base pairs. *RNA.* 2001; 7(4):499–512. [PubMed: 11345429]
- Liberman JA, Wedekind JE. Riboswitch structure in the ligand-free state. *Wiley interdisciplinary reviews. RNA.* 2011
- Liu JD, Zhao L, Xia T. The dynamic structural basis of differential enhancement of conformational stability by 5'- and 3'-dangling ends in RNA. *Biochemistry.* 2008; 47(22):5962–5975. [PubMed: 18457418]
- Loenen WA. S-adenosylmethionine: jack of all trades and master of everything? *Biochemical Society transactions.* 2006; 34(Pt 2):330–333. [PubMed: 16545107]
- Lu J, Kadakkuzha BM, Zhao L, Fan M, Qi X, Xia T. Dynamic ensemble view of the conformational landscape of HIV-1 TAR RNA and allosteric recognition. *Biochemistry.* 2011; 50(22):5042–5057. [PubMed: 21553929]
- Mahen EM, Watson PY, Cottrell JW, Fedor MJ. mRNA secondary structures fold sequentially but exchange rapidly in vivo. *PLoS biology.* 2010; 8(2):e1000307. [PubMed: 20161716]
- Mandal M, Boese B, Barrick JE, Winkler WC, Breaker RR. Riboswitches control fundamental biochemical pathways in *Bacillus subtilis* and other bacteria. *Cell.* 2003; 113(5):577–586. [PubMed: 12787499]
- Mandal M, Breaker RR. Adenine riboswitches and gene activation by disruption of a transcription terminator. *Nature structural & molecular biology.* 2004a; 11(1):29–35.
- Mandal M, Breaker RR. Gene regulation by riboswitches. *Nature reviews. Molecular cell biology.* 2004b; 5(6):451–463. [PubMed: 15173824]
- McDaniel BA, Grundy FJ, Artsimovitch I, Henkin TM. Transcription termination control of the S box system: direct measurement of S-adenosylmethionine by the leader RNA. *Proceedings of the National Academy of Sciences of the United States of America.* 2003; 100(6):3083–3088. [PubMed: 12626738]
- Merino EJ, Wilkinson KA, Coughlan JL, Weeks KM. RNA structure analysis at single nucleotide resolution by selective 2'-hydroxyl acylation and primer extension (SHAPE). *Journal of the American Chemical Society.* 2005; 127(12):4223–4231. [PubMed: 15783204]
- Meyer MM, Roth A, Chervin SM, Garcia GA, Breaker RR. Confirmation of a second natural preQ1 aptamer class in Streptococcaceae bacteria. *RNA.* 2008; 14(4):685–695. [PubMed: 18305186]
- Mironov AS, Gusarov I, Rafikov R, Lopez LE, Shatalin K, Kreneva RA, Perumov DA, Nudler E. Sensing small molecules by nascent RNA: a mechanism to control transcription in bacteria. *Cell.* 2002; 111(5):747–756. [PubMed: 12464185]
- Montange RK, Batey RT. Structure of the S-adenosylmethionine riboswitch regulatory mRNA element. *Nature.* 2006; 441(7097):1172–1175. [PubMed: 16810258]
- Moore T, Zhang Y, Fenley MO, Li H. Molecular basis of box C/D RNA-protein interactions; cocrystal structure of archael L7Ae and a box C/D RNA. *Structure.* 2004; 12(5):807–818. [PubMed: 15130473]
- Mulhbacher J, Brouillet E, Allard M, Fortier LC, Malouin F, Lafontaine DA. Novel riboswitch ligand analogs as selective inhibitors of guanine-related metabolic pathways. *PLoS pathogens.* 2010; 6(4):e1000865. [PubMed: 20421948]
- Mulhbacher J, Lafontaine DA. Ligand recognition determinants of guanine riboswitches. *Nucleic acids research.* 2007; 35(16):5568–5580. [PubMed: 17704135]

- Murphy FL, Cech TR. GAAA tetraloop and conserved bulge stabilize tertiary structure of a group I intron domain. *Journal of molecular biology*. 1994; 236(1):49–63. [PubMed: 8107125]
- Nahvi A, Sudarsan N, Ebert MS, Zou X, Brown KL, Breaker RR. Genetic control by a metabolite binding mRNA. *Chemistry & biology*. 2002; 9(9):1043. [PubMed: 12323379]
- Neuman KC, Nagy A. Single-molecule force spectroscopy: optical tweezers, magnetic tweezers and atomic force microscopy. *Nature methods*. 2008; 5(6):491–505. [PubMed: 18511917]
- Neupane K, Yu H, Foster DA, Wang F, Woodside MT. Single-molecule force spectroscopy of the adenosine riboswitch relates folding to regulatory mechanism. *Nucleic acids research*. 2011
- Nissen P, Ippolito JA, Ban N, Moore PB, Steitz TA. RNA tertiary interactions in the large ribosomal subunit: the A-minor motif. *Proceedings of the National Academy of Sciences of the United States of America*. 2001; 98(9):4899–4903. [PubMed: 11296253]
- Noeske J, Buck J, Furtig B, Nasiri HR, Schwalbe H, Wohner J. Interplay of 'induced fit' and preorganization in the ligand induced folding of the aptamer domain of the guanine binding riboswitch. *Nucleic acids research*. 2007; 35(2):572–583. [PubMed: 17175531]
- Noeske J, Richter C, Grundl MA, Nasiri HR, Schwalbe H, Wohner J. An intermolecular base triple as the basis of ligand specificity and affinity in the guanine- and adenine-sensing riboswitch RNAs. *Proceedings of the National Academy of Sciences of the United States of America*. 2005; 102(5): 1372–1377. [PubMed: 15665103]
- Omer AD, Ziesche S, Ebhardt H, Dennis PP. In vitro reconstitution and activity of a C/D box methylation guide ribonucleoprotein complex. *Proceedings of the National Academy of Sciences of the United States of America*. 2002; 99(8):5289–5294. [PubMed: 11959980]
- Ott E, Stoltz J, Lehmann M, Mack M. The RFN riboswitch of *Bacillus subtilis* is a target for the antibiotic roseoflavin produced by *Streptomyces davawensis*. *RNA biology*. 2009; 6(3):276–280. [PubMed: 19333008]
- Ottink OM, Rampersad SM, Tessari M, Zaman GJ, Heus HA, Wijmenga SS. Ligand-induced folding of the guanine-sensing riboswitch is controlled by a combined predetermined induced fit mechanism. *RNA*. 2007; 13(12):2202–2212. [PubMed: 17959930]
- Pan T, Sosnick T. RNA folding during transcription. *Annual review of biophysics and biomolecular structure*. 2006; 35:161–175.
- Peters JM, Vangeloff AD, Landick R. Bacterial transcription terminators: the RNA 3'-end chronicles. *Journal of molecular biology*. 2011; 412(5):793–813. [PubMed: 21439297]
- Pikovskaya O, Polonskaia A, Patel DJ, Serganov A. Structural principles of nucleoside selectivity in a 2'-deoxyguanosine riboswitch. *Nature chemical biology*. 2011
- Proshkin S, Rahmouni AR, Mironov A, Nudler E. Cooperation between translating ribosomes and RNA polymerase in transcription elongation. *Science*. 2010; 328(5977):504–508. [PubMed: 20413502]
- Prychyna O, Dahabieh MS, Chao J, O'Neill MA. Sequence-dependent folding and unfolding of ligand-bound purine riboswitches. *Biopolymers*. 2009; 91(11):953–965. [PubMed: 19603494]
- Ray PS, Jia J, Yao P, Majumder M, Hatzoglou M, Fox PL. A stress-responsive RNA switch regulates VEGFA expression. *Nature*. 2009; 457(7231):915–919. [PubMed: 19098893]
- Regulski EE, Breaker RR. In-line probing analysis of riboswitches. *Methods in molecular biology*. 2008; 419:53–67. [PubMed: 18369975]
- Regulski EE, Moy RH, Weinberg Z, Barrick JE, Yao Z, Ruzzo WL, Breaker RR. A widespread riboswitch candidate that controls bacterial genes involved in molybdenum cofactor and tungsten cofactor metabolism. *Molecular microbiology*. 2008; 68(4):918–932. [PubMed: 18363797]
- Rieder R, Lang K, Gruber D, Micura R. Ligand-induced folding of the adenosine deaminase A-riboswitch and implications on riboswitch translational control. *Chembiochem : a European journal of chemical biology*. 2007; 8(8):896–902. [PubMed: 17440909]
- Rieder U, Lang K, Kreutz C, Polacek N, Micura R. Evidence for pseudoknot formation of class I preQ1 riboswitch aptamers. *Chembiochem : a European journal of chemical biology*. 2009; 10(7):1141–1144. [PubMed: 19382115]
- Ross P, Weinhouse H, Aloni Y, Michaeli D, Weinberger-Ohana P, Mayer R, Braun S, De Vroom E, Van DER, Marel GA, Van Boom JH, Benziman M. Regulation of cellulose synthesis in

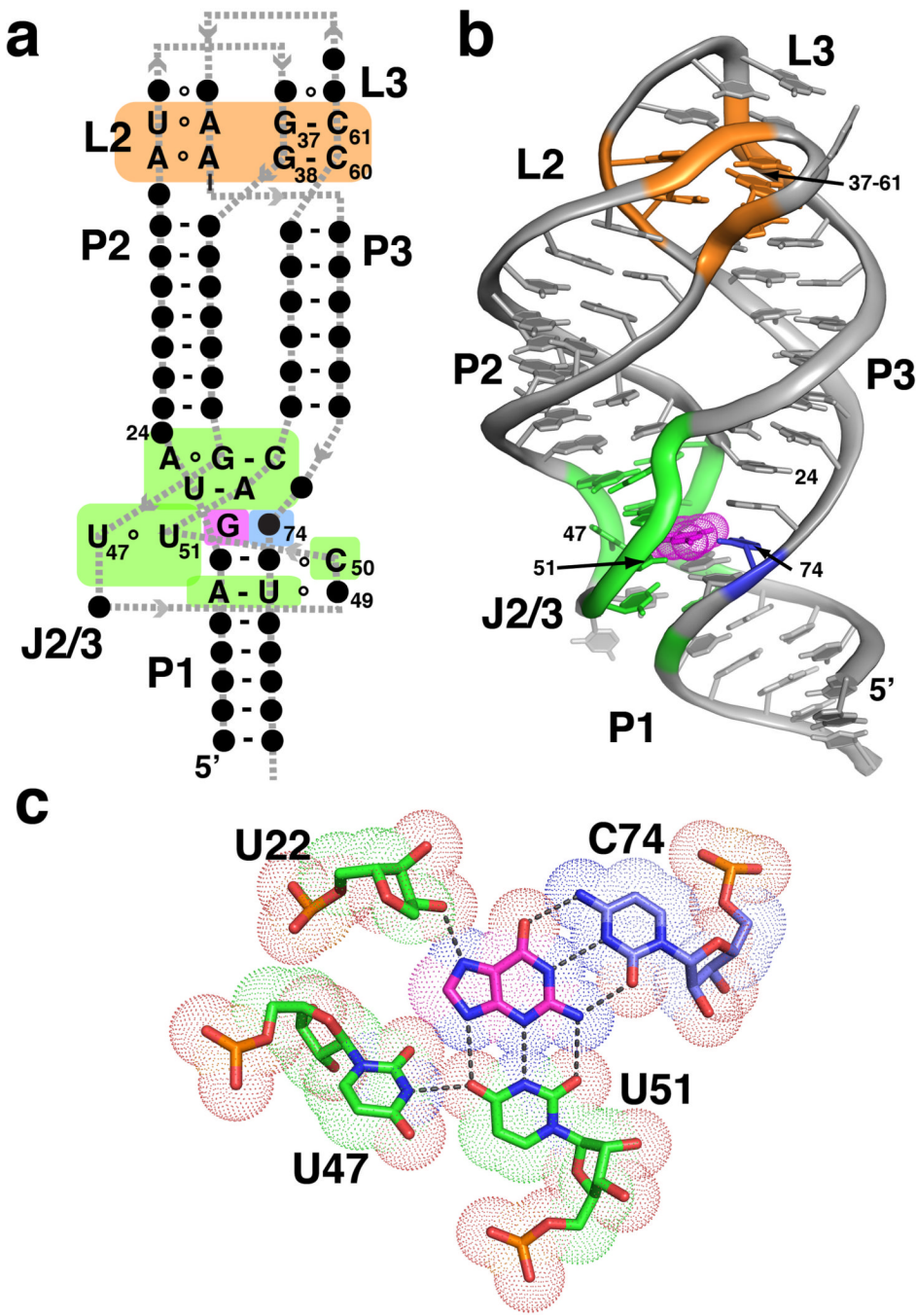
- Acetobacter xylinum by cyclic diguanylic acid. *Nature*. 1987; 325(6101):279–281. [PubMed: 18990795]
- Roth A, Winkler WC, Regulski EE, Lee BW, Lim J, Jona I, Barrick JE, Ritwik A, Kim JN, Welz R, Iwata-Reuy D, Breaker RR. A riboswitch selective for the queuosine precursor preQ1 contains an unusually small aptamer domain. *Nature structural & molecular biology*. 2007; 14(4):308–317.
- Ryjenkov DA, Simm R, Romling U, Gomelsky M. The PilZ domain is a receptor for the second messenger c-di-GMP: the PilZ domain protein YcgR controls motility in enterobacteria. *The Journal of biological chemistry*. 2006; 281(41):30310–30314. [PubMed: 16920715]
- Saran D, Frank J, Burke DH. The tyranny of adenosine recognition among RNA aptamers to coenzyme A. *BMC evolutionary biology*. 2003; 3:26. [PubMed: 14687414]
- Sassanfar M, Szostak JW. An RNA motif that binds ATP. *Nature*. 1993; 364(6437):550–553. [PubMed: 7687750]
- Saxild HH, Brunstedt K, Nielsen KI, Jarmer H, Nygaard P. Definition of the *Bacillus subtilis* PurR operator using genetic and bioinformatic tools and expansion of the PurR regulon with glyA, guaC, pbuG, xpt-pbuX, yqhZ-fold, and pbuO. *Journal of bacteriology*. 2001; 183(21):6175–6183. [PubMed: 11591660]
- Sazani PL, Larralde R, Szostak JW. A small aptamer with strong and specific recognition of the triphosphate of ATP. *Journal of the American Chemical Society*. 2004; 126(27):8370–8371. [PubMed: 15237981]
- Schroeder R, Barta A, Semrad K. Strategies for RNA folding and assembly. *Nature reviews. Molecular cell biology*. 2004; 5(11):908–919. [PubMed: 15520810]
- Serganov A, Yuan YR, Pikovskaya O, Polonskaia A, Malinina L, Phan AT, Hobartner C, Micura R, Breaker RR, Patel DJ. Structural basis for discriminative regulation of gene expression by adenine- and guanine-sensing mRNAs. *Chemistry & biology*. 2004; 11(12):1729–1741. [PubMed: 15610857]
- Shajani Z, Sykes MT, Williamson JR. Assembly of bacterial ribosomes. *Annual review of biochemistry*. 2011; 80:501–526.
- Shanahan CA, Gaffney BL, Jones RA, Strobel SA. Differential analog binding by two classes of c-di-GMP riboswitches. *Journal of the American Chemical Society*. 2011
- Shimotsu H, Kuroda MI, Yanofsky C, Henner DJ. Novel form of transcription attenuation regulates expression the *Bacillus subtilis* tryptophan operon. *Journal of bacteriology*. 1986; 166(2):461–471. [PubMed: 2422155]
- Silverman SK. Rube Goldberg goes (ribo)nuclear? Molecular switches and sensors made from RNA. *RNA*. 2003; 9(4):377–383.
- Sinha J, Reyes SJ, Gallivan JP. Reprogramming bacteria to seek and destroy an herbicide. *Nature chemical biology*. 2010a; 6(6):464–470.
- Sinha J, Reyes SJ, Gallivan JP. Reprogramming bacteria to seek and destroy an herbicide. *Nature chemical biology*. 2010b; 6(6):464–470.
- Sinha J, Topp S, Gallivan JP. From SELEX to cell dual selections for synthetic riboswitches. *Methods in enzymology*. 2011; 497:207–220. [PubMed: 21601088]
- Smith KD, Lipchock SV, Ames TD, Wang J, Breaker RR, Strobel SA. Structural basis of ligand binding by a c-di-GMP riboswitch. *Nature structural & molecular biology*. 2009; 16(12):1218–1223.
- Smith KD, Lipchock SV, Livingston AL, Shanahan CA, Strobel SA. Structural and biochemical determinants of ligand binding by the c-di-GMP riboswitch. *Biochemistry*. 2010; 49(34):7351–7359. [PubMed: 20690679]
- Smith KD, Shanahan CA, Moore EL, Simon AC, Strobel SA. Structural basis of differential ligand recognition by two classes of bis-(3'-5')-cyclic dimeric guanosine monophosphate-binding riboswitches. *Proceedings of the National Academy of Sciences of the United States of America*. 2011; 108(19):7757–7762. [PubMed: 21518891]
- Souliere MF, Haller A, Rieder R, Micura R. A powerful approach for the selection of 2-aminopurine substitution sites to investigate RNA folding. *Journal of the American Chemical Society*. 2011; 133(40):16161–16167. [PubMed: 21882876]

- Spitale RC, Torelli AT, Krucinska J, Bandarian V, Wedekind JE. The structural basis for recognition of the PreQ0 metabolite by an unusually small riboswitch aptamer domain. *The Journal of biological chemistry*. 2009; 284(17):11012–11016. [PubMed: 19261617]
- Staple DW, Butcher SE. Pseudoknots: RNA structures with diverse functions. *PLoS biology*. 2005; 3(6):e213. [PubMed: 15941360]
- Stelzer AC, Frank AT, Kratz JD, Swanson MD, Gonzalez-Hernandez MJ, Lee J, Andrecioaei I, Markovitz DM, Al-Hashimi HM. Discovery of selective bioactive small molecules by targeting an RNA dynamic ensemble. *Nature chemical biology*. 2011; 7(8):553–559.
- Stoddard CD, Gilbert SD, Batey RT. Ligand-dependent folding of the three-way junction in the purine riboswitch. *RNA*. 2008; 14(4):675–684. [PubMed: 18268025]
- Stoddard CD, Montange RK, Hennelly SP, Rambo RP, Sanbonmatsu KY, Batey RT. Free state conformational sampling of the SAM-I riboswitch aptamer domain. *Structure*. 2010; 18(7):787–797. [PubMed: 20637415]
- Storz G, Vogel J, Wassarman KM. Regulation by Small RNAs in Bacteria: Expanding Frontiers. *Molecular cell*. 2011; 43(6):880–891. [PubMed: 21925377]
- Sudarsan N, Cohen-Chalamish S, Nakamura S, Emilsson GM, Breaker RR. Thiamine pyrophosphate riboswitches are targets for the antimicrobial compound pyrithiamine. *Chemistry & biology*. 2005; 12(12):1325–1335. [PubMed: 16356850]
- Sudarsan N, Lee ER, Weinberg Z, Moy RH, Kim JN, Link KH, Breaker RR. Riboswitches in eubacteria sense the second messenger cyclic di-GMP. *Science*. 2008; 321(5887):411–413. [PubMed: 18635805]
- Thomas JR, Hergenrother PJ. Targeting RNA with small molecules. *Chemical reviews*. 2008; 108(4): 1171–1224. [PubMed: 18361529]
- Tomsic J, McDaniel BA, Grundy FJ, Henkin TM. Natural variability in Sadenosylmethionine (SAM)-dependent riboswitches: S-box elements in bacillus subtilis exhibit differential sensitivity to SAM In vivo and in vitro. *Journal of bacteriology*. 2008; 190(3):823–833. [PubMed: 18039762]
- Trausch JJ, Ceres P, Reyes FE, Batey RT. The structure of a tetrahydrofolate-sensing riboswitch reveals two ligand binding sites in a single aptamer. *Structure*, A.O.P. 2011
- Turnbough CL JR, Switzer RL. Regulation of pyrimidine biosynthetic gene expression in bacteria: repression without repressors. *Microbiology and molecular biology reviews : MMBR*. 2008; 72(2):266–300. table of contents. [PubMed: 18535147]
- Vicens Q, Cech TR. Atomic level architecture of group I introns revealed. *Trends in biochemical sciences*. 2006; 31(1):41–51. [PubMed: 16356725]
- Vicens Q, Mondragon E, Batey RT. Molecular sensing by the aptamer domain of the FMN riboswitch: a general model for ligand binding by conformational selection. *Nucleic acids research*. 2011
- Vinayak M, Pathak C. Queuosine modification of tRNA: its divergent role in cellular machinery. *Biosci Rep*. 2010; 30(2):135–148. [PubMed: 19925456]
- Vitreschak AG, Rodionov DA, Mironov AA, Gelfand MS. Riboswitches: the oldest mechanism for the regulation of gene expression? *Trends in genetics : TIG*. 2004; 20(1):44–50. [PubMed: 14698618]
- Voth AR, Hays FA, Ho PS. Directing macromolecular conformation through halogen bonds. *Proceedings of the National Academy of Sciences of the United States of America*. 2007; 104(15):6188–6193. [PubMed: 17379665]
- Wang KC, Chang HY. Molecular mechanisms of long noncoding RNAs. *Molecular cell*. 2011; 43(6): 904–914. [PubMed: 21925379]
- Weeks KM, Mauger DM. Exploring RNA Structural Codes with SHAPE Chemistry. *Accounts of chemical research*. 2011
- Weill L, Louis D, Sargeuil B. Selection and evolution of NTP-specific aptamers. *Nucleic acids research*. 2004; 32(17):5045–5058. [PubMed: 15452272]
- Weinberg Z, Barrick JE, Yao Z, Roth A, Kim JN, Gore J, Wang JX, Lee ER, Block KF, Sudarsan N, Neph S, Tompa M, Ruzzo WL, Breaker RR. Identification of 22 candidate structured RNAs in bacteria using the CMfinder comparative genomics pipeline. *Nucleic acids research*. 2007; 35(14):4809–4819. [PubMed: 17621584]

- Weinberg Z, Wang JX, Bogue J, Yang J, Corbino K, Moy RH, Breaker RR. Comparative genomics reveals 104 candidate structured RNAs from bacteria, archaea, and their metagenomes. *Genome biology*. 2010; 11(3):R31. [PubMed: 20230605]
- Wickiser JK, Cheah MT, Breaker RR, Crothers DM. The kinetics of ligand binding by an adenine-sensing riboswitch. *Biochemistry*. 2005a; 44(40):13404–13414. [PubMed: 16201765]
- Wickiser JK, Winkler WC, Breaker RR, Crothers DM. The speed of RNA transcription and metabolite binding kinetics operate an FMN riboswitch. *Molecular cell*. 2005b; 18(1):49–60. [PubMed: 15808508]
- Wilkinson KA, Merino EJ, Weeks KM. RNA SHAPE chemistry reveals nonhierarchical interactions dominate equilibrium structural transitions in tRNA(Asp) transcripts. *Journal of the American Chemical Society*. 2005; 127(13):4659–4667. [PubMed: 15796531]
- Wilkinson KA, Merino EJ, Weeks KM. Selective 2'-hydroxyl acylation analyzed by primer extension (SHAPE): quantitative RNA structure analysis at single nucleotide resolution. *Nature protocols*. 2006; 1(3):1610–1616.
- Winkler WC, Breaker RR. Genetic control by metabolite-binding riboswitches. *Chembiochem : a European journal of chemical biology*. 2003; 4(10):1024–1032. [PubMed: 14523920]
- Winkler WC, Grundy FJ, Murphy BA, Henkin TM. The GA motif: an RNA element common to bacterial antitermination systems, rRNA, and eukaryotic RNAs. *RNA*. 2001; 7(8):1165–1172. [PubMed: 11497434]
- Woodside MT, Garcia-Garcia C, Block SM. Folding and unfolding single RNA molecules under tension. *Current opinion in chemical biology*. 2008; 12(6):640–646. [PubMed: 18786653]
- Xayaphoummine A, Viasnoff V, Harlepp S, Isambert H. Encoding folding paths of RNA switches. *Nucleic acids research*. 2007; 35(2):614–622. [PubMed: 17178750]
- Yarus M. Getting past the RNA world: the initial Darwinian ancestor. *Cold Spring Harbor perspectives in biology*. 2011; 3(4)
- Zemora G, Waldsch C. RNA folding in living cells. *RNA biology*. 2010; 7(6):634–641. [PubMed: 21045541]
- Zhang J, Lau MW, Ferre-D'Amare AR. Ribozymes and riboswitches: modulation of RNA function by small molecules. *Biochemistry*. 2010; 49(43):9123–9131. [PubMed: 20931966]
- Zhao L, Xia T. Direct revelation of multiple conformations in RNA by femtosecond dynamics. *Journal of the American Chemical Society*. 2007; 129(14):4118–4119. [PubMed: 17373794]
- Zhao L, Xia T. Probing RNA conformational dynamics and heterogeneity using femtosecond time-resolved fluorescence spectroscopy. *Methods*. 2009; 49(2):128–135. [PubMed: 19362148]

**Figure 1.**

A typical riboswitch that regulates transcription. (top) Binding of the effector ligand binding to the aptamer domain (AD, green) fates the expression platform (EP, yellow) to form a rho-independent transcriptional terminator. This stem-loop structure causes RNAP to disengage from mRNA synthesis, thereby turning off expression. (bottom) In the absence of ligand binding to the aptamer, the P1 helix is destabilized and the “switching sequence” is available to form the competing antiterminator structure disrupts formation of the terminator as well, allowing for full transcription of the mRNA.

**Figure 2.**

Structure of the guanine riboswitch. (a) Secondary structure of the guanine riboswitch. Only nucleotide positions whose identity is >97% conserved across all phylogenetic variants are presented; all other nucleotide positions are denoted as dark circles. Canonical Watson-Crick base pairing interactions are shown by dashes, noncanonical pairs are denoted by open circles, and the backbone trace is given through the grey dashed line. Paired regions are denoted by “P” (P1 – P3 in this case), terminal hairpin loops by “L” (L2 and L3), and joining regions by “J” (J2/3). This convention will be used throughout all the figures in this review. Regions of interest are shaded: the binding pocket is colored green, the specificity pyrimidine is cyan, and the two base quadruples that establish the L2–L3 interaction is

orange. (b) Tertiary structure of the guanine riboswitch aptamer domain bound to guanine (PDB ID 1Y27). The shaded regions reflect those in part (a). (c) Guanine recognition is effected through a base triple with two universally conserved pyrimidine residues (U51 and C74). The specificity pyrimidine is shown in blue (74) and is a uridine in all adenine responsive variants. The dots, representing the van der Waals surface of the atoms highlight that the nucleobase is almost entirely surrounded by RNA.

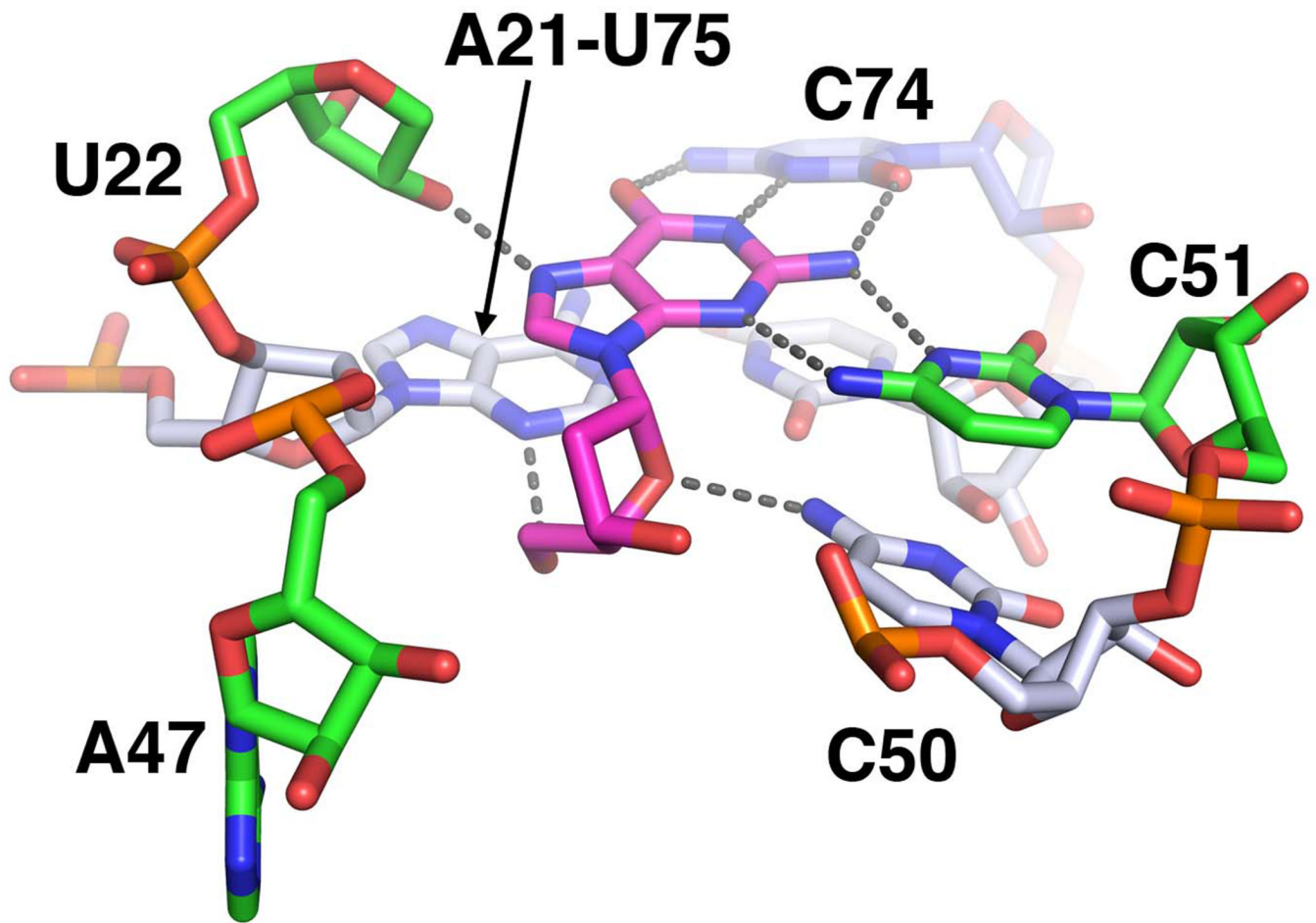
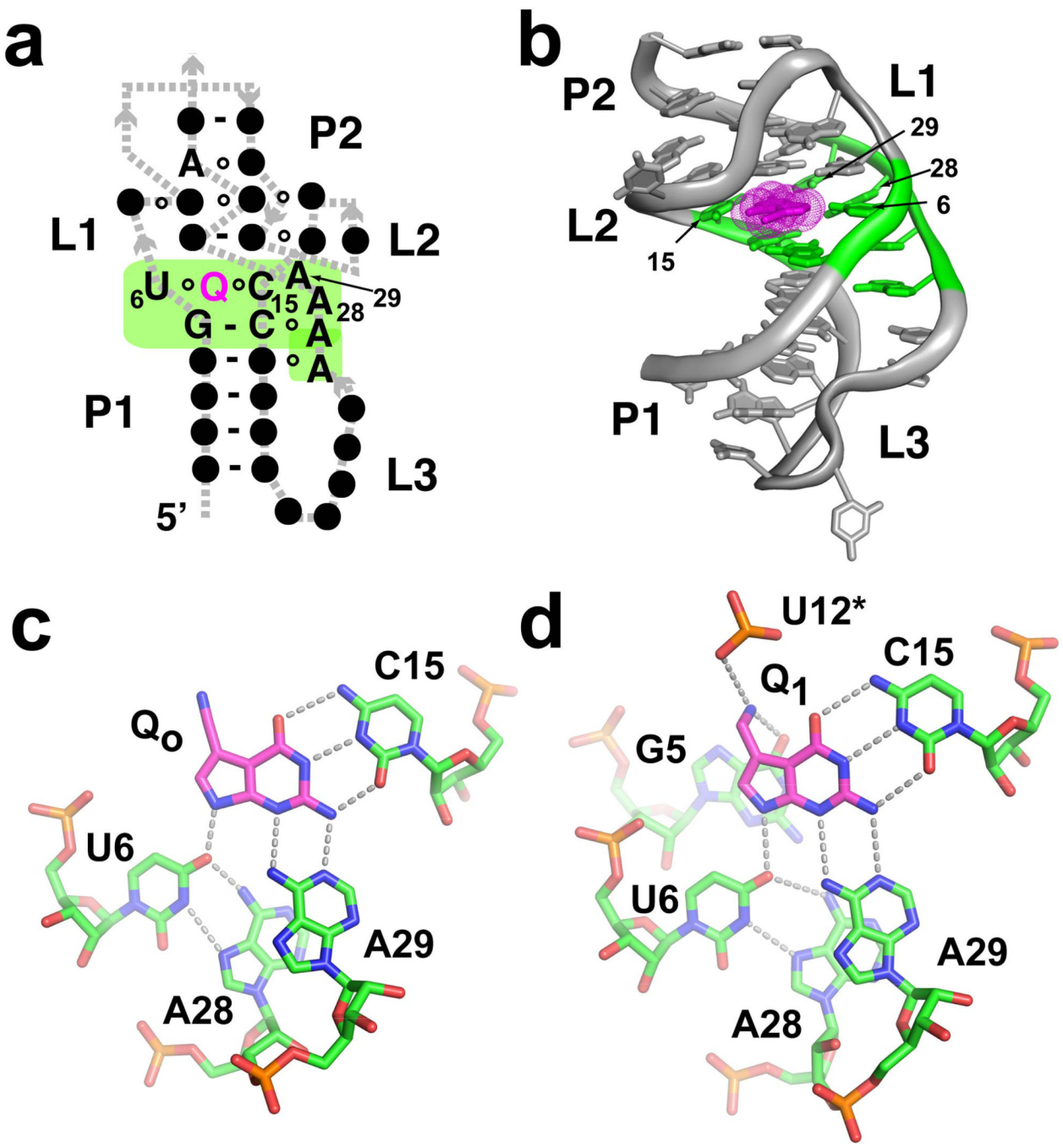
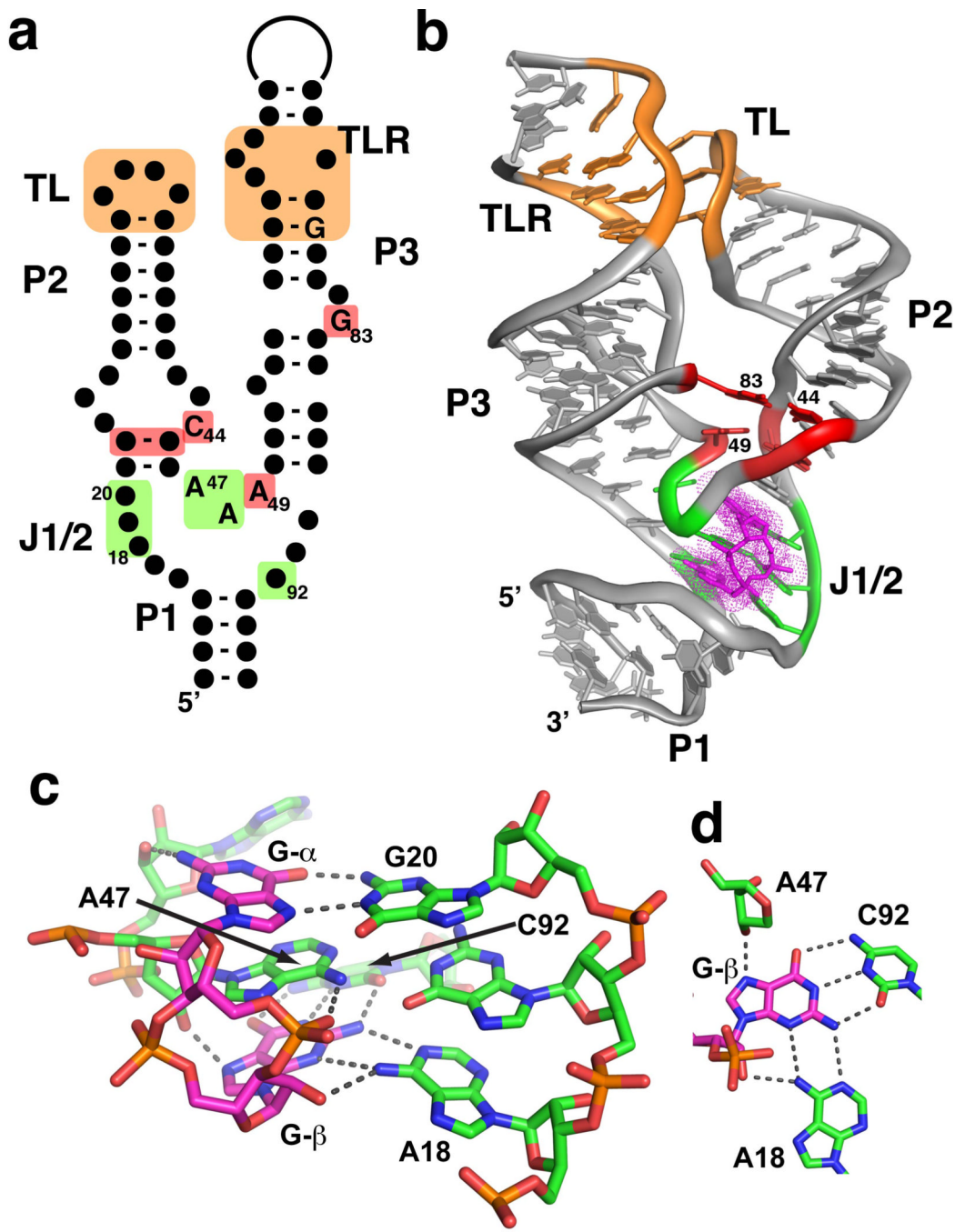


Figure 3.

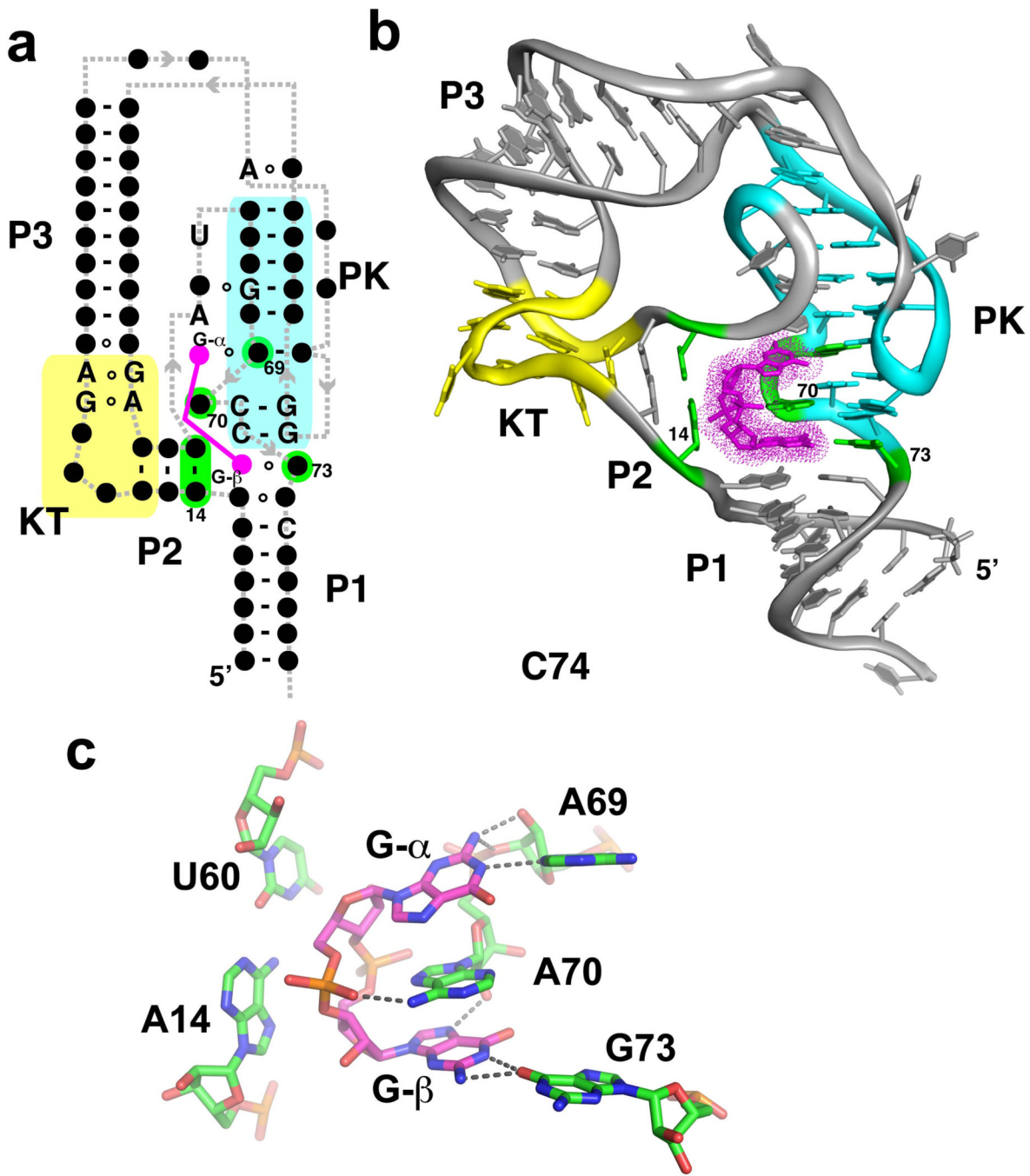
Recognition of 2'-deoxyguanosine by the purine (PDB ID 3DS7). The nucleobase moiety hydrogen bonds to C51 and C74; note that C51 is shifted towards C74 relative to the guanine riboswitch to provide room for the 2'-deoxyribose moiety. To further accommodate the sugar, A47 is shifted away from C51 (compare to Fig. 2c). Further interactions with the sugar are made with the adjacent base triple in P1.

**Figure 4.**

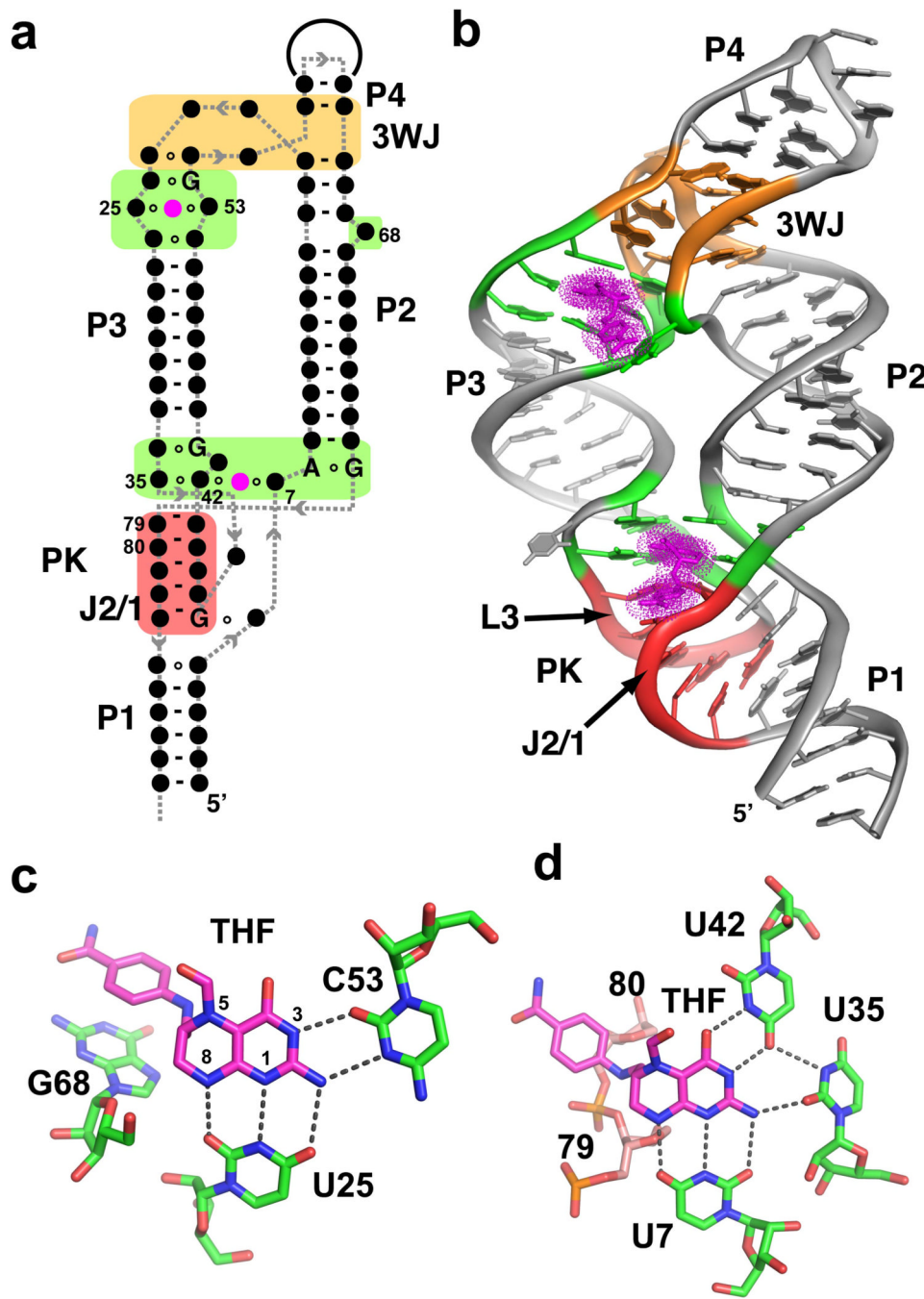
Structure of the preQ₁-I riboswitch aptamer. (a) Secondary structure of the aptamer domain. The binding site for preQ₁ (magenta "Q") is shaded in green. (b) Tertiary structure of the *Thermoanaerobacter tengcongensis* preQ₁ aptamer in complex with Q₀ (PDB ID 3GCA). (c) Recognition of Q₀ by the *T. tengcongensis* aptamer. Note a hydrogen bonding pattern very similar to that of the purine riboswitch (Fig. 2c). (d) Recognition of Q₁ by the *B. subtilis* preQ₁ riboswitch aptamer domain (type II; PDB ID 3FU2), emphasizing additional hydrogen bonding interactions that give rise to the riboswitch's preference for Q₁ over Q₀ and guanine.

**Figure 5.**

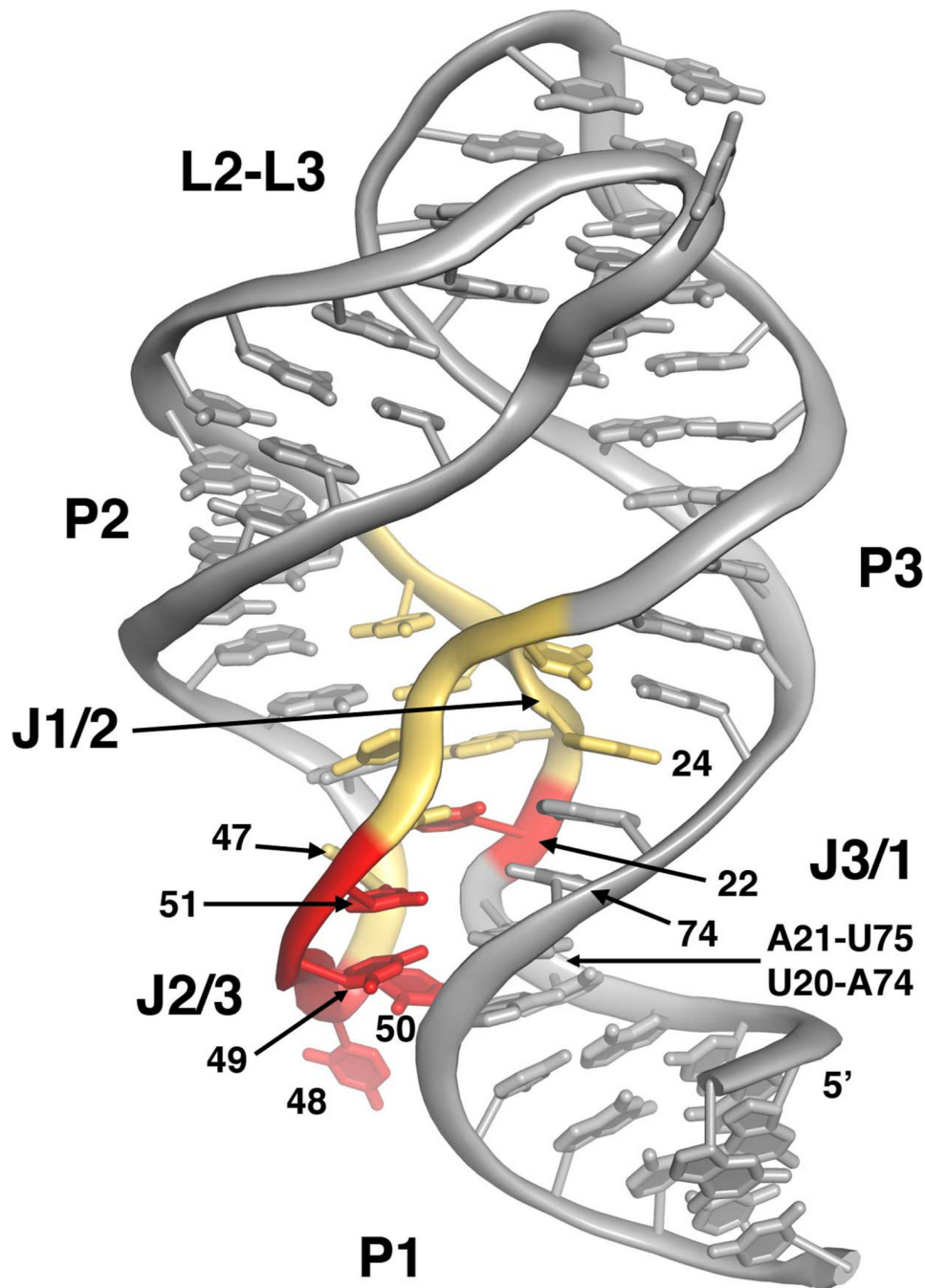
Structure of the class I cyclic-di-GMP riboswitch aptamer. (a) Secondary structure of the aptamer domain. The binding site is shaded green, the tetraloop-tetraloop receptor (TL-TLR) is shown in orange, and a second conserved set of tertiary interactions that serve to anchor P2 and P3 together in red. (b) Tertiary structure of the ligand-aptamer complex (PDB ID 3IRW). (c) Recognition of c-di-GMP by the three way junction of the aptamer, emphasizing the hydrogen bonding network between the ligand and RNA. (d) Another view of the recognition of G β of c-di-GMP by the aptamer.

**Figure 6.**

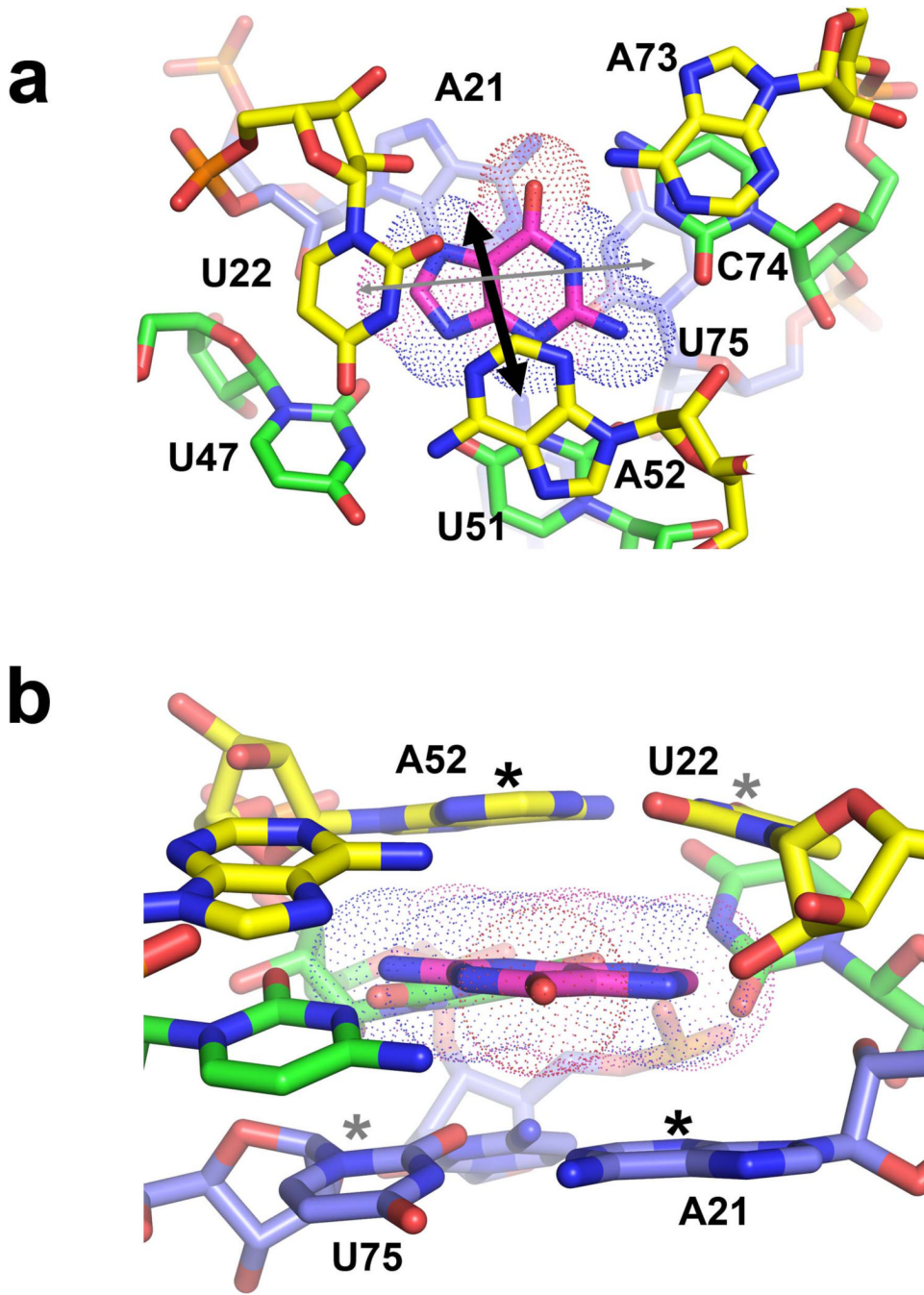
Structure of the class II cyclic-di-GMP riboswitch aptamer. (a) Secondary structure of the aptamer. The binding site is shaded in green, the pseudoknot in cyan, and the kink-turn (KT) in yellow. (b) Tertiary structure of the aptamer (PDB ID 3Q3Z). (c) Recognition of cyclic-di-GMP by the riboswitch. Note that the mode of recognition of both G- α and G- β is very different from the class I riboswitch, but in both cases an adenine intercalates between the guanosine residues.

**Figure 7.**

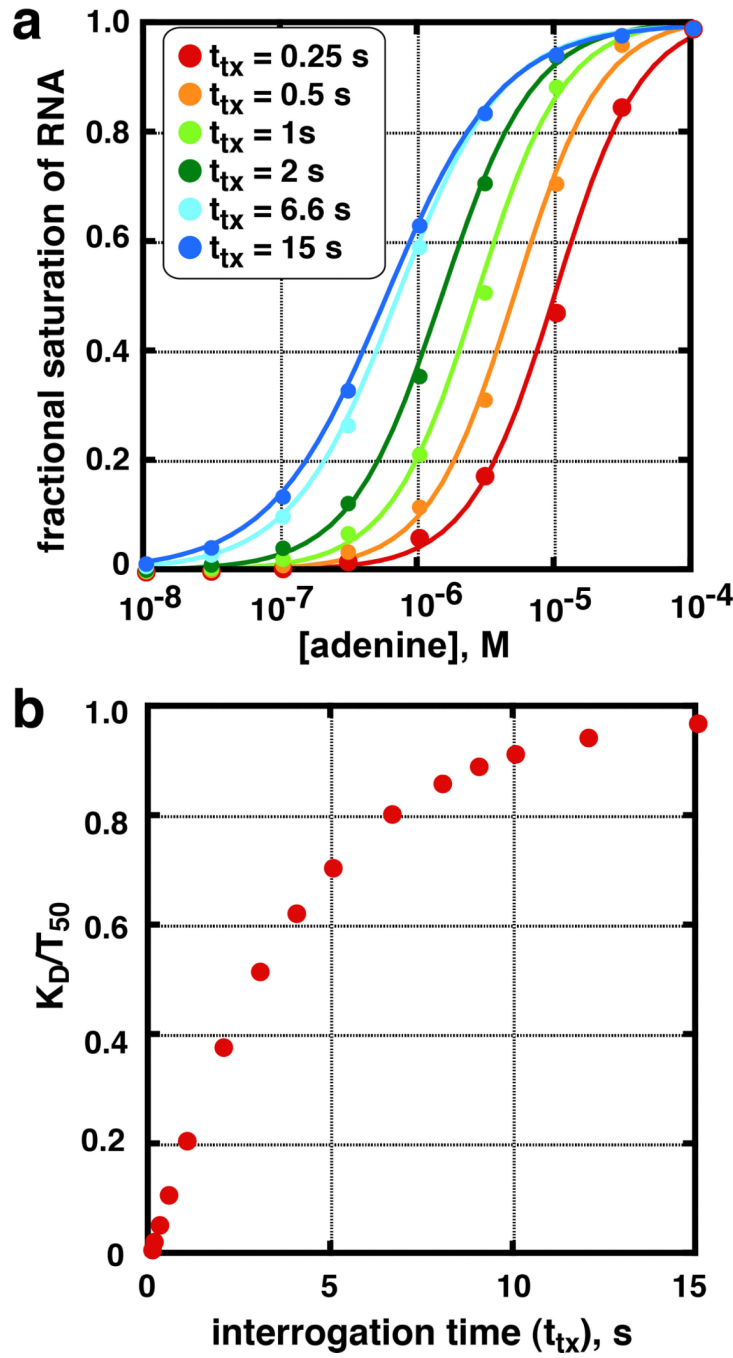
Structure of the tetrahydrofolate (THF) riboswitch aptamer. (a) Secondary structure of the THF riboswitch aptamer domain, highlighting the two separate THF binding sites (green), the three-way junction (3WJ, orange), and the pseudoknot (PK, red). Note that only a few nucleotides are universally conserved in this aptamer, none of which directly contact the ligands. (b) Tertiary structure of the THF aptamer (PDB ID 3SD1). (c) Recognition of THF by the three-way junction site. (d) Recognition of THF by the pseudoknot site.

**Figure 8.**

Structure of the *xpt* guanine riboswitch colored by the $\Delta T_{m,app}$ of each nucleotide as measured by SHAPE chemical probing. The $\Delta T_{m,app}$ is the difference between the $T_{m,app}$ measured in the presence of 10 μM hypoxanthine and in the absence of hypoxanthine. Nucleotide positions with a $\Delta T_{m,app} < 10^\circ\text{C}$ are grey, $10^\circ\text{C} < \Delta T_{m,app} < 20^\circ\text{C}$ are colored yellow, and $\Delta T_{m,app} > 20^\circ\text{C}$ are red. Note that the only nucleotide outside of J2/3 that has a large ligand dependent shift in its $T_{m,app}$ is U22, whose 2'-hydroxyl group directly participates in a hydrogen bond with the N7 of the purine nucleobase (see Fig. 2c).

**Figure 9.**

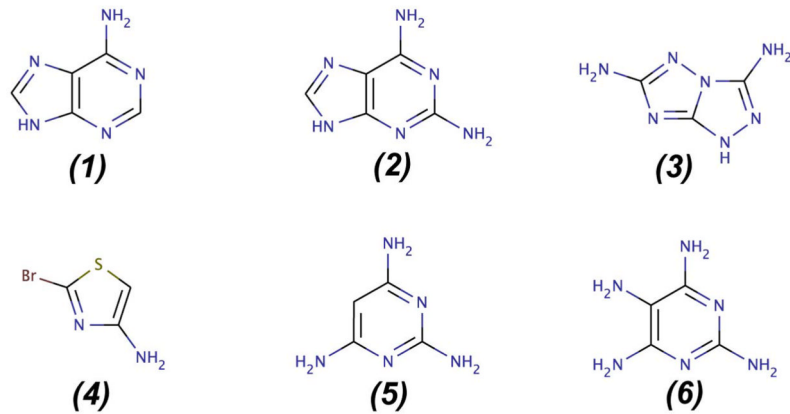
Elastic motions of the purine nucleobase as measured by fast fluorescence spectroscopy. (a) Base triples above and below the binding pocket (Fig. 2c) are represented by yellow and blue carbons, respectively. The majority of the population (~60%) was assigned as that observed in the crystal structure in which the nucleobase is not stacked between the A21–U75 and U22–A52 base pairs. A second population (~30%) was found to be stacked with A21 and/or A52 (thick black arrow) and a third minor population (~10%) is stacked with U22 or U75 (thin grey arrow). (b) Side view of the binding pocket with the bases upon which the ligand transiently stack highlighted by asterisks.

**Figure 10.**

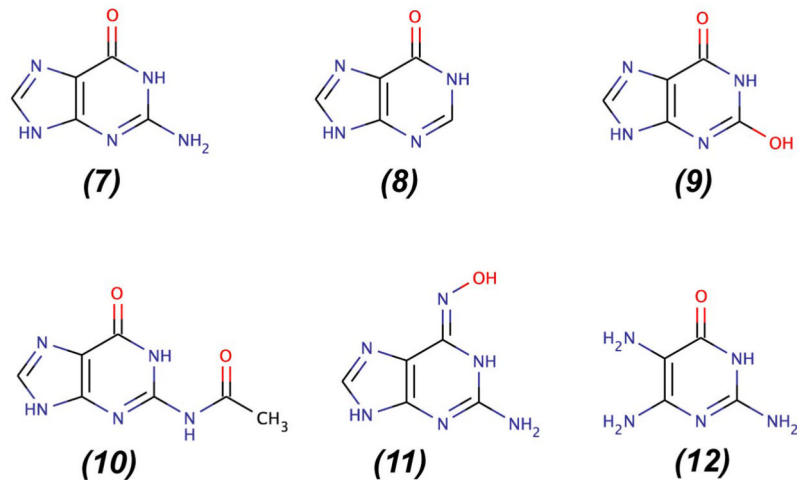
Modeling of thermodynamic and kinetic control of riboswitches. (a) Regulatory response curves as a function of adenine concentration as given by equation (2). Each curve represents a specific time required to transcribe the message from the end of the aptamer domain ($t=0$) until completion of the intrinsic terminator (decision point, t_{tx}). The curves are calculated using the published values for the association and dissociation rate for the pbuE adenine riboswitch at 35 °C and 1×10^{-12} M for the RNA concentration (Wickiser et al., 2005a). For these values, $t = 6.6$ seconds represents $1/k_{off}$, and the curve for $t = 15$ seconds is nearly identical to that calculated for $t = \infty$. (b) The data from (a) transformed to yield a direct correlation between the T_{50} and the time the aptamer domain has to equilibrate with

the cellular environment (interrogation time). K_D/T_{50} is the ratio of the measured affinity of the aptamer domain at equilibrium and the calculated concentration of adenine required to elicit a half maximal regulatory response (the fit of the curves in panel (a)). As t_{tx} increases, this ratio reaches the asymptotic limit of 1, which reflects the aptamer being able to equilibrate during t_{tx} . It has been suggested that a K_D/T_{50} value of 0.75 be considered the boundary between the kinetic control ($K_D/T_{50} < 0.75$) and thermodynamic control ($K_D/T_{50} > 0.75$).

a. Adenine riboswitch binding compounds



b. Guanine riboswitch binding compounds



c. Compounds that bind both riboswitches

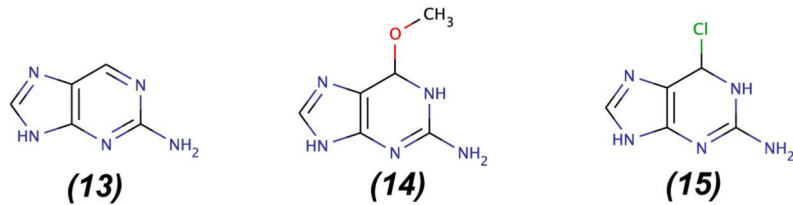


Figure 11.

Compounds able to bind to the guanine/adenine classes of the purine riboswitch. (a) Compounds that bind the adenine riboswitch include adenine (1), 2,6-diaminopurine (2), 1,2,4-triazolo-1,2,4-triazole-3,6-diamine (3), 3-bromo-1,2,4-thiadiazol-5-amine (4), 2,4,6-triamino-1,3,5-triazine (5), 2,4,5,6-tetraaminopyrimidine (6). (b) Compounds that bind the guanine riboswitch include guanine (7), hypoxanthine (8), the enol tautomer of xanthine (9), 2-acetoamido-6-hydroxypurine (10), 6-N-hydroxylaminopurine (11), and 2,5,6-triaminopyrimidin-4-one (12). (c) Compounds that bind both riboswitches are 2-aminopurine (13), 6-O-methylguanine (14), and 6-chloroguanine (15).

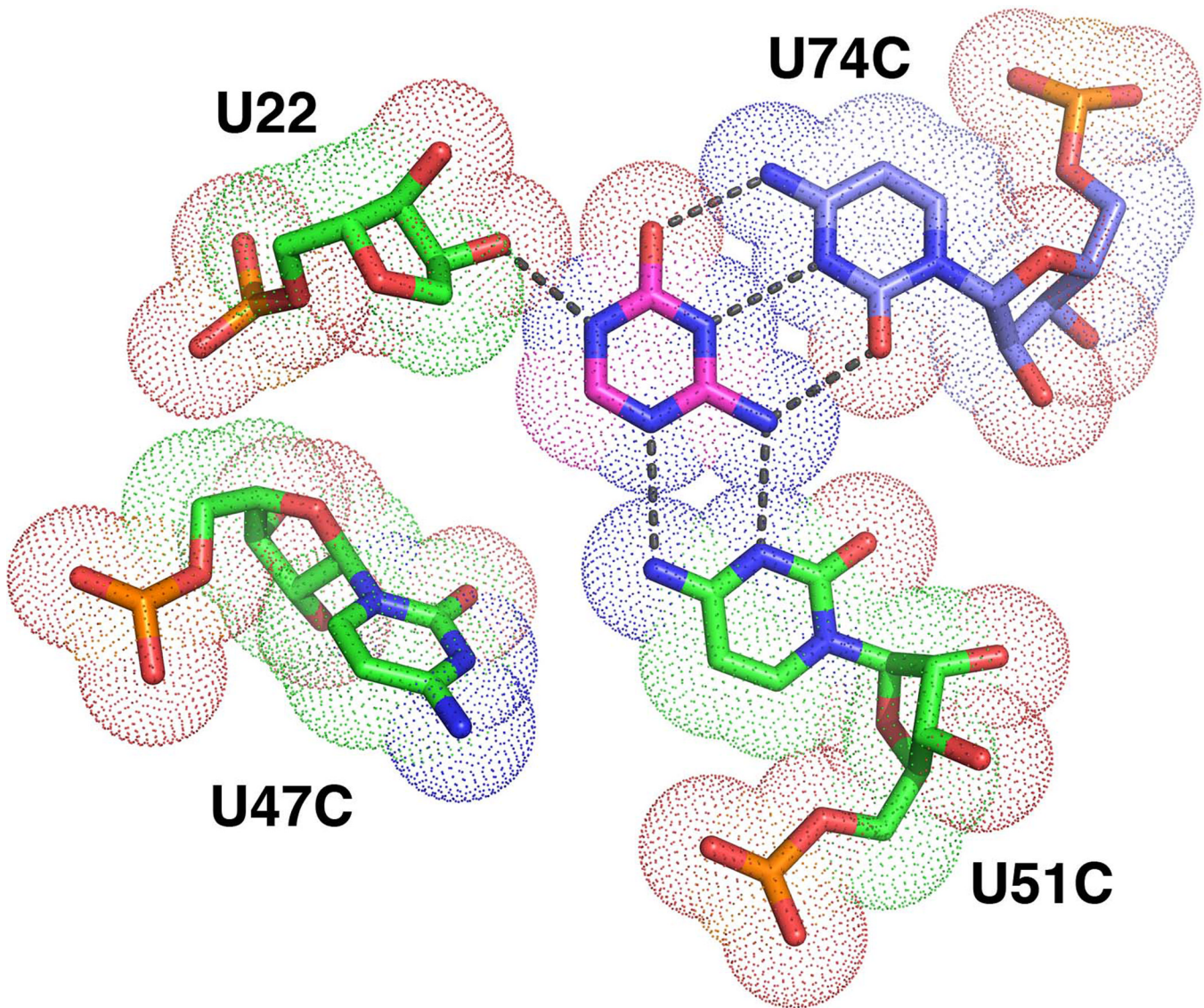


Figure 12.

Crystal structure of azacytosine bound to the engineered binding pocket of the *add* adenine riboswitch containing a U47C/U51C/U74C mutations (PDB ID 3LA5). Other mutations were introduced at the base of the P2 helix to further increase the RNA's affinity for azacytosine.